ISTANBUL TECHNICAL UNIVERSITY ★ GRADUATE SCHOOL OF SCIENCE ENGINEERING AND TECHNOLOGY

SURGE PRESSURE PREDICTION USING HERSCHEL-BULKLEY RHEOLOGICAL MODEL AND COMPARISON OF ANALYTICAL AND LANDMARK SOFTWARE RESULTS

M.Sc. THESIS

Muhammad Mubeen ur Rehman ARAIN

Department of Petroleum and Natural Gas Engineering

Petroleum and Natural Gas Engineering Programme

JUNE 2015

ISTANBUL TECHNICAL UNIVERSITY ★ GRADUATE SCHOOL OF SCIENCE ENGINEERING AND TECHNOLOGY

SURGE PRESSURE PREDICTION USING HERSCHEL-BULKLEY RHEOLOGICAL MODEL AND COMPARISON OF ANALYTICAL AND LANDMARK SOFTWARE RESULTS

M.Sc. THESIS

Muhammad Mubeen ur Rehman ARAIN
(505121508)

Department of Petroleum and Natural Gas Engineering

Petroleum and Natural Gas Engineering Programme

Thesis Advisor: Asst. Prof. Dr. Gürşat ALTUN

JUNE 2015

İSTANBUL TEKNİK ÜNİVERSİTESİ ★ FEN BİLİMLERİ ENSTİTÜSÜ

HERSHEL-BULKLEY MODELİ KULLANILARAK SURGE BASINÇLARININ TAHMİNİ VE SONUÇLARIN ANALİTİK VE YAZILIM KARŞILAŞTIRILMASI

YÜKSEK LİSANS TEZİ

Muhammad Mubeen ur Rehman ARAIN
(505121508)

Petrol ve Doğal Gaz Mühendisliği Anabilim Dalı

Petrol ve Doğal Gaz Mühendisliği Programı

Tez Danışmanı: Yrd. Doç. Dr. Gürşat ALTUN

HAZIRAN 2015

Muhammad Mubeen ur Rehman Arain, a **M.Sc.** student of ITU **Graduate School of Science, Engineering and Technology** student ID **505121508**, successfully defended the **thesis** entitled "**SURGE PRESSURE PREDICTION USING HERSCHEL-BULKLEY RHEOLOGICAL MODEL AND COMPARISON OF ANALYTICAL AND LANDMARK SOFTWARE RESULTS**", which he prepared after fulfilling the requirements specified in the associated legislations,

Thesis Advisor :	**Asst. Prof. Dr. Gürşat ALTUN** Istanbul Technical University	.....
Jury Members :	**Asst. Prof. Dr. Ibrahim Metin MIHÇAKAN** Istanbul Technical University	.....
	Assoc. Prof. Dr. Cemal BALCI Istanbul Technical University	.....

Date of Submission : 04 May 2015
Date of Defense : 03 June 2015

FOREWORD

I would like to express my sincere gratitude and appreciation to my supervisor Asst. Prof. Dr. Gursat Altun for his consistent support all through the study duration. His valuable guidance and inspiration always helped me enhancing both academically and personally.

I am grateful to Asst. Prof. Dr. Senol Yamanlar for his efforts to keep software program active and accessible in the computer laboratory.

I also would like to thank Research Asst. Mr. Ali Ettehadi Osgouei for his assistance in laboratory work. His cooperation and useful suggestions remained a source of encouragement for me.

It has been a wonderful experience for me to study in the Department of Petroleum and Natural Gas Engineering at the Istanbul Technical University.

May 2015

Muhammad Mubeen Arain

Petroleum and Natural Gas Engineer

TABLE OF CONTENTS

Page

ABBREVIATIONS

ROP	**:** Rate of Penetration
NPT	**:** Non Productive Time
ERD	**:** Extended Reach Drilling
SPP	**:** Stand Pipe Pressure
HWDP	**:** Heavy Weight Drill pipe
RIH	**:** Run in Hole
HTHP	**:** High Temperature and High Pressure
POOH	**:** Pull Out of Hole
TFA	**:** Total Flow Area
JIF	**:** Jet Impact Force
ESD	**:** Equivalent Static Density
HB	**:** Herschel-Bulkley
UWSM	**:** Unweighted Sepiolite Mud
WSM	**:** Weighted Sepiolite Mud
KCL	**:** Potassium Chloride

NOMENCLATURE

$\boldsymbol{n}$	**:** Flow behaviour index
K	**:** Consistency index, Pa.s
γ	**:** Shear rate, s^{-1}
$\boldsymbol{\tau}$	**:** Shear stress, Pa or lb.f/sq.ft
μ	**:** Newtonian viscosity, dyne.s/cm^2 or poise
$\boldsymbol{\tau_o}$ ***or*** $\boldsymbol{\tau_y}$	**:** Yield point or Yield stress, Pa or lb.f/sq.ft
μ_p	**:** Plastic viscosity, Pa.s or cP
$\overline{\boldsymbol{v}}$	**:** Effective fluid velocity, ft/s
$\boldsymbol{v_{(ie)}}$	**:** Effective fluid velocity inside pipe, ft/s or m/s
$\boldsymbol{v_{ae}}$	**:** Effective fluid velocity inside annulus, ft/s or m/s
$\boldsymbol{C_d}$	**:** Bit discharge coefficient, %
$\boldsymbol{C_c}$	**:** Correction coefficient for pipe section
$\boldsymbol{C_a}$	**:** Correction coefficient for annular section
q_p	**:** Flow rate inside pipe, ft^3/s
q_a	**:** Flow rate inside annulus, ft^3/s
$\boldsymbol{A_j}$	**:** Bit discharge area, sq.in. or sq.m
$\Delta \boldsymbol{p_b}$	**:** Pressure drop at bit, psi
$\boldsymbol{f_a}$	**:** Fractional flow in annulus
$\boldsymbol{\rho}$	**:** Fluid density, lbm/gal

v_p	**:** Trip speed, ft/s
f	**:** Fanning friction factor
R_e	**:** Reynolds number
$R_{e\,eq}$	**:** Equivalent Reynolds number
$R_{e\,eqcr}$	**:** Critical equivalent Reynolds number
L	**:** Length, ft or m
Δp	**:** Pressure drop, psi or bar
Q	**:** Flow rate, ft^3/s or m^3/s
R	**:** Inside drillpipe radius, ft
R_1	**:** Inner radius of annulus, ft
R_2	**:** Outer radius of annulus, ft
V_p	**:** Fluid velocity in pipe, ft/s or m/s
V_a	**:** Fluid velocity in annulus, ft/s or m/s

Subscripts

i	**:** Inside pipe
a	**:** Inside annulus
b	**:** Bit
t	**:** Total
dp	**:** Drillpipe
dc	**:** Drillcollar

LIST OF TABLES

Page

LIST OF FIGURES

Page

SURGE PRESSURE PREDICTION USING HERSCHEL-BULKLEY RHEOLOGICAL MODEL AND COMPARISON OF ANALYTICAL AND LANDMARK SOFTWARE RESULTS

SUMMARY

In drilling hydraulics, the estimation of surge and swab pressures is important due to the fact that, the excessive surge pressures generated by pipe movement in tripping operations may result in serious consequences such as blowout and formation damage. Tripping operation can be performed due to several reasons such as adding pipe stand to drillstring, changing worn bit, removing fallen parts from borehole (fishing) or running logging tools. The time spent in tripping operation is a significant portion of the total time spent during overall drilling operations. During the drilling of offshore wells in deep waters, extended reach drilling (ERD) wells and highly deviated wells, small margins are encountered between pore pressure and formation fracture pressure. In such cases, the proper prediction of surge and swab pressure may exhibit paramount importance in order to ensure trouble free and cost effective drilling operations. In this work, the method for estimating surge pressures by analytical calculations using Herschel-Bulkley rheological model is presented and the results are compared with those obtained from Paradigm Sysdrill software, version 10.

In calculating the frictional pressure losses for Herschel-Bulkley model the equations introduced by Merlo, et al. (1995) are employed. The barite-weighted and unweighted fresh water sepiolite muds are used in this study. The results estimated with Sysdrill software shows discrepancy, and the surge pressures are lower as compare to the results taken from analytical model. The surge pressures are also estimated using Bingham Plastic and Power Law model, and results are compared with Herschel-Bulkley rheological model.

Additionally, a sensitivity analysis is performed to investigate the major parameters that affect surge pressures. The effect of tripping speed and fluid density exhibits the direct relationship, while the effect of borehole clearance exhibits the inverse relationship to the surge pressures. The study shows that, upto the certain degree of temperature, the surge pressures decrease with the increase in formation temperature, and then afterwards the surge pressures display an increment. For better understanding of formation temperature effect on mud rheology and surge pressures, the rheological constants for the mentioned mud samples are taken, using both Fann35A rotational viscometer and Fann50SL high temperature and high pressure (HTHP) rheometer. It is also determined that at the formation temperature up to 350°F, the use of both weighted and unweighted sepiolite muds allow to fasten the tripping speed of the drillstring.

HERSHEL-BULKLEY MODELİ KULLANILARAK SURGE BASINÇLARININ TAHMİNİ VE SONUÇLARIN ANALİTİK VE YAZILIM KARŞILAŞTIRILMASI

ÖZET

Yeraltı enerji kaynakaları araştırması (petrol, gaz ve jeotermal) dünya enerji gereksinimini karşılamaya bağlı olarak artmaktadır. Günümüzde teknik olarak doğru ve maliyeti düşük sondaj uygulamaları çok kritik bir hale gelmiştir. Son birkaç on yılda, kuyu hidroliği büyük dikkat çekmiş ve buna bağlı olarak yüksek eğimli kuyular, uzun erişimli ve yatay kuyuların sayısında büyük artış görülmektedir. Bu sondaj ortamlarında formasyon basıncı ve formasyon çatlatma gradyeni arasındaki operasyonel pencere veya açıklık marjini genel olarak daha azdır ve sondaj dizisinin kuyu içerisine veya kuyudan dışarıya doğru olan manevrası sırasında meydana gelen kuyu içi basınç değişimlerinin veya dalgalanmalarının (surge veya swab olarak bilinmektedir) doğru bir şekilde tahmin edilmesi gerektiğini yansıtmaktadır. Sondaj akışkanının aşağı ve yukarı hareketinden kaynaklanan ve kuyu içi basınç dalgalanması (surge veya swab) olarak bilinen bu basınç değişimleri genellikle sürtünme basınç kayıplarıdır. Sondaj dizisi kuyu dışına doğru çekildiği zaman kuyudaki akışkanı akışkanı yukarıya doğru sürükler (drag), bu nedenle kuyu dibinde hidrostatik basınçta swab olarak bilinen bir basınç azalmasına sebep olur. Bunun tersi harekette, dizi kuyu içerisinde aşağı doğru hareket ettirildiğinde akışkanı aşağı doğru sürükler ve surge olarak bilinen kuyu içi basıncının artmasına neden olur. Sondaj dizisinin manevra operasyonu diziye boru eklemek, aşınmış matkabı değiştirmek, kuyu içerisinde kalmış parçaları dışarı çıkarmak (tahlisiye operasyonu) veya kuyu ölçüm aletlerinin (log aletleri) kuyuya indirilmesi ve çıkarılması gibi nedenlerle yapılır. Manevra operasyonlarında harcanan zaman genel olarak tüm sondaj zamanı için harcanan zamanın önemli bir bölümünü oluşturur. Manevra nedeniyle oluşan bu basınçların doğru bir şekilde belirlenmesi ve bilinmesi, sorunların azaltılmasında ve düşük maliyetli etkin bir sondaj operasyonunun yapılmasında çok büyük bir önemi vardır.

Manevra nedeniyle oluşan kuyu içi basınç dalgalanmalarının (surge ve swab basınçları) hesaplanması sondaj hidroliğinde çok önemlidir. Sondaj dizisinin manevrası nedeniyle oluşabilecek yüksek basınç dalgalanmaları formasyon hasarı ve kuyu fışkırmaları gibi çok ciddi sorunlara neden olabilir. Formasyon basıncı ve formasyon çatlatma basıncı arasındaki açıklığın genel olarak küçük olduğu derindeniz kuyularının, uzun erişimli kuyuların (ERD) ve yüksek açılı kuyuların sondajı sırasında basınç dalgalanmalarının uygun bir şekilde tahmini önemi yadsınamaz bir gerçektir. Bu çalışmada, dizi hareketinden kaynaklanan basınç dalgalanmalarını hesaplayan yöntem Herschel-Bulkley akışkan modeli kullanılarak sunulmuştur ve sonuçlar Paradigm Sysdrill yazılımı (V.10) ile karşılaştırılmıştır. Çalışmada, basınç dalgalanmalarını bulmak için Merlo vd. (1995) tarafından tanıtılan sürtünme basınç kayıplarını Herschel-Bulkley akışkan için hesaplayan analitik denklemler kullanılmıştır.

Sondaj dizisinin manevrası nedeniyle oluşan basınçların (surge ve swab) Herschel-Bulkley analitik modeli kullanılarak çözümü literatürde günümüze kadar yayınlanmamıştır ve bu yönüyle bu çalışma bir ilktir. Ancak, bu model denklemleri kullanılarak sondaj akışkanının sirkülasyonu sırasında meydana gelen sürtünme basınç kayıplarının (stand pipe pressure) belirlenmesine yönelik çalışmalar yayınlanmıştır. Çalışmada yapılan hesaplamalarda kuyunun düşey olduğu, kuyu anülüsünde dizinin merkezi olduğu (konsentrik), sondaj çamurunun sıkıştırılamaz akışkan olduğu ve kararlı akış durumları kabul edilmiştir.

Ticari yazılım olan Paradigm Sysdrill (v.10) simülatörü sondaj kuyusunun planlanmasında, yön kontrolünde ve sondaj mühendisliği analizlerinde yaygın bir şekilde kullanılmaktadır. Bu program iki önemli modülden oluşmaktadır; bunlar (1) Sysdrill kuyu planlama ve yön kontrolü ve (2) Sysdrill sondaj mühendisliği. Bu çalışmada Sysdrill yazılımı Herschel-Bulkley modeli kullanılarak analitik olarak çözülen problem sonuçlarını karşılaştırmak için kullanılmıştır. Yazılımın dizi hareketi nedeniyle oluşan kuyu içi basınç dalgalanmalarını yanlış hesapladığı (sadece Herschel-Bulkley model değil, aynı zamanda Bingham Plastik ve Power Law gibi diğer reolojik modelleri içinde) belirlenmiştir. Konu hakkında yazılım firmasıyla irtibata geçilmiş ve programın yeni versiyonunda bu hatanın giderileceği bilgisi teyit edilmiştir.

Barit-ağırlaştırılmış ve ağırlaştırılmamış su bazlı sepiolit çamurlar çalışmada kullanılmıştır. Sysdril yazılımından tahmin edilen sonuçlar farklılık göstermiştir ve kuyu içi basınç dalgalanmaları değerleri analitik model sonuçlarından alınanlara göre daha düşüktür. Kuyuiçi basınç dalgalanmaları (surge basınçları) Bingham Plastik ve Power Law reolojik modelleri kullanılarakta tahmin edilmiş ve sonuçlar Herschel-Bulkley model sonuçlarıyla karşılaştırılmıştır.

Ayrıca, bu basınç dalgalanması üzerine etki eden parametreleri incelemek için duyarlılık analizi de gerçekleştirilmiştir. Kuyuiçi basınç dalgalanmaları dizi manevra hızı ve akışkan yoğunluğu ile doğrusal bir ilişki etkisi gösterirken, kuyu açıklığı (borehole clearance) doğrusal olmayan bir ilişki göstermiştir. Çalışma göstermiştir ki, kuyu içi basınç dalgalanması belli bir sıcaklık değerine kadar artan sıcaklıkla azalırken, daha sonra bu sıcaklıktan yüksek sıcaklıklarda basınç değerlerinde bir artış göstermiştir. Formasyon sıcaklığının çamur reolojisi ve kuyu içi basınç dalgalanması üzerine olan etkisini daha iyi anlayabilmek için belirtilen çamur örneklerinin reolojik sabitleri hem Fann35A döner viskometre hem de Fann50SL yüksek sıcaklık ve yüksek basınç (YSYB) reometresi kullanılarak ölçülmüştür. Sıcaklık koşullarını daha doğru canlandıran reometre ölçümlerinden elde edilen sonuçların viskometre sonuçlarından oldukça farklı değerler verdiği belirlenmiştir. Yüksek sıcaklıklı kuyuların analizinde viskometreden elde edilen sonuçlara göre yapılacak olan mühendislik analizlerinin yanlışlıklara ve dolayısıyla istenmeyen sorunlara neden olabileceği de gösterilmiştir. 350°F formasyon sıcaklığına kadar hem ağırlaştırılmış hem de ağırlaştırılmamış sepiolit çamurlarının sondaj dizisinin manevra hızlarının artırılmasına izin verdiği de belirlenmiştir. Bunula birlikte, doğru manevra hızlarının belirlenebilmesi için reometreye dayalı reolojik sabitlerin belirlenmesi gerekmektedir.

Çalışmadan elde edilen diğer önemli sonuçlar aşağıda özet olarak verilmektedir:

- Herschel-Bulkley modelinin analitik çözümü sonuçlarından elde edilen kuyu içi basınç dalgalanmaları (surge/swab) ticari yazılımın sonuçlarından daha iyi

sonuç vermektedir. Analitik çözüm sonuçları daha yüksektir ve sonuçlar daha korunaklı ve güvenlikli bir çözüm vermektedir.

- Kuyu içi basınç dalgalanmalarının artışına neden olan en önemli parametre manevra sırasındaki dizi hızının değeridir. Artan dizi hızıyla birlikte bu basınçlarda artmaktadır.

- Kuyu içi basınç dalgalanmaları artan çmaur yoğunluğuyla birlikte artmaktadır, ancak artış oranı dizi hızındaki kadar yüksek değildir.

- Dizi ve formasyon arasındaki anüler açıklık ile basınç dalgalanma değeri arasında ters bir ilişki vardır ve artan anüler açıklıkla birlikte basınç dalgalanmaları hızlı bir şekilde düşmektedir.

- Hem barit-ağırlaştırılmış hem de ağırlaştırılmamış sepiolit temelli sondaj akışkanı durumunda, formasyon sıcaklığının dolayısı ile sondaj akışkanının belli bir değerine kadar (çamur jelleşmesi etkisi görülünceye kadar olan sıcaklık artışları) kuyu içi basınç dalgalanma (surge ve swab) değerlerinde azalma görülmektedir ve bu sıcaklık eşiğine (350° F) kadar manevra hızları arttırılabilir.

- Sıcaklık ile birlikte değişen sondaj akışkanının reolojik sabitlerinin kuyu içi basınç dalgalanmaları (surge/swab) değerleri üzerine büyük etkisi vardır.

- Sürtünme basınç kayıplarını daha doğru tahmin etmek için Herschel-Bulkley modelini göz önüne alan çamur yapışma sabiti (mud clinging constant) denklemleri ve/veya grafikleri günümüze kadar geliştirilmemiş ve literatürde yoktur. Bu nedenle, çalışmada Power Law akışkan için geliştirilmiş olan denklemler kullanılmıştır.

- Yüksek sıcaklık koşullarında bütün özellikleri reometreden belirlenen sadece sepiolit temelli çamur özellikleri bu çalışmada kullanılmıştır. Diğer çamur türleri için (KCL, polimer temelli çamurlar, Lignosülfonat gibi) bu çalışma tekraralanabilir ve sepiolit çamur sonuçlarıyla karşılaştırılabilir.

1. INTRODUCTION

Exploitation of underground energy resourses (oil, natural gas and geothermal) has been increasing with the acute demand for fulfilling world energy requirements. Proper and cost effective drilling practices are of cruitial importance nowadays. In the past few decades, wellbore hydraulics has received great attention, so long as drilling of highly deviated, extended reach, and horizontal wells have shown rapid growth. In such drilling environment the operational window between pore pressure and formation fracture gradient is having narrow margin, which reflects the importance of predicting accurate downhole pressure fluctuations that might be caused by either tripping in or tripping out of drillstring or reciprocation of casing in borehole. These pressure fluctuations, which are usually the frictional pressure drop resulting from the upward or downward motion of drilling fluid are known as surge or swab pressure. When pulling out of hole the movement of drillstring drags the borehole fluid upward and, thus causes a decrease in bottom hole pressure, known as swab pressure. On the contrary when running in the hole the movement of drillstring drags the borehole fluid downward and causes an increase in bottom hole pressure, known as surge pressure. Accurate knowledge of these pressures is of great importance in ensuring trouble free drilling operations. The Herschel-Bulkley (HB) rheological model, or yield-power law model, usually gives the best fit for the viscometer data or best describes the rheology of mostly used drilling and completion fluids, compared to the other rheological models of Bingham plastic or Power law model (Merlo et al., 1995).

1.1 Drilling Hydraulics

During a drilling operation the hydraulic system plays an active role, in the sense that its proper design can accelerate the rate of penetration (ROP) and lower the overall drilling cost. Few of the frequent and time consuming operations during drilling are the running of pipe string, tripping the bit and running casing or liner string in the hole. In Table 1.1, the time analysis for drilling rig is given and it can be seen that,

the time spent in tripping operation is a significant portion of the total time spent during overall drilling operations.

Table 1.1 : Rig time analysis for tendered rig (Bourgoyne, 1991).

Drilling Operation	Total Time Required (hours)	Time Fraction
Drilling	351	0.17
Tripping	388	0.19
Rigging up	348	0.17
Formation evaluation and borehole surveys	103	0.05
Casing placement	199	0.10
Well completion	211	0.10
Drilling problems	450	0.22
Mud conditioning	143	
Well control operation	12	
Fishing operation	152	
Severe weather	97	
Rig repairs	20	
Logistics	26	
Total	**2050**	**1.00**

When a pipe string is pulled out of hole at fast speed to save time, fluid motion may generate significant swab pressures in the hole and may result in well kick. On the other hand, if pipe is run with fast speed, the fluid motion may generate large surge pressures, that may result in fracturing of formation or loss of circulation.

Figure 1.1 gives a schematic of a rig circulating system that can be divided into four sections in terms of calculating pressure losses:

a) Surface connection losses are those taking place in standpipe, rotary hose, swivel and kelly. The magnitude of these losses are dependent on the dimension and geometry of the mentioned equipments.

b) Pressure losses occur inside the drillpipes, heavy weight drillpipes (HWDP), and drillcollars.

c) Pressure losses occur in the annular section of the borehole, that is outside of drillpipes, HWDP, and drillcollars. The magnitude of losses descirbed in b) and c), depends on the dimension of these pipes (inside or outside diameter and length), mud rheological properties (mud weight, plastic viscosity, and yield point) and type of flow (laminar or turbulent).

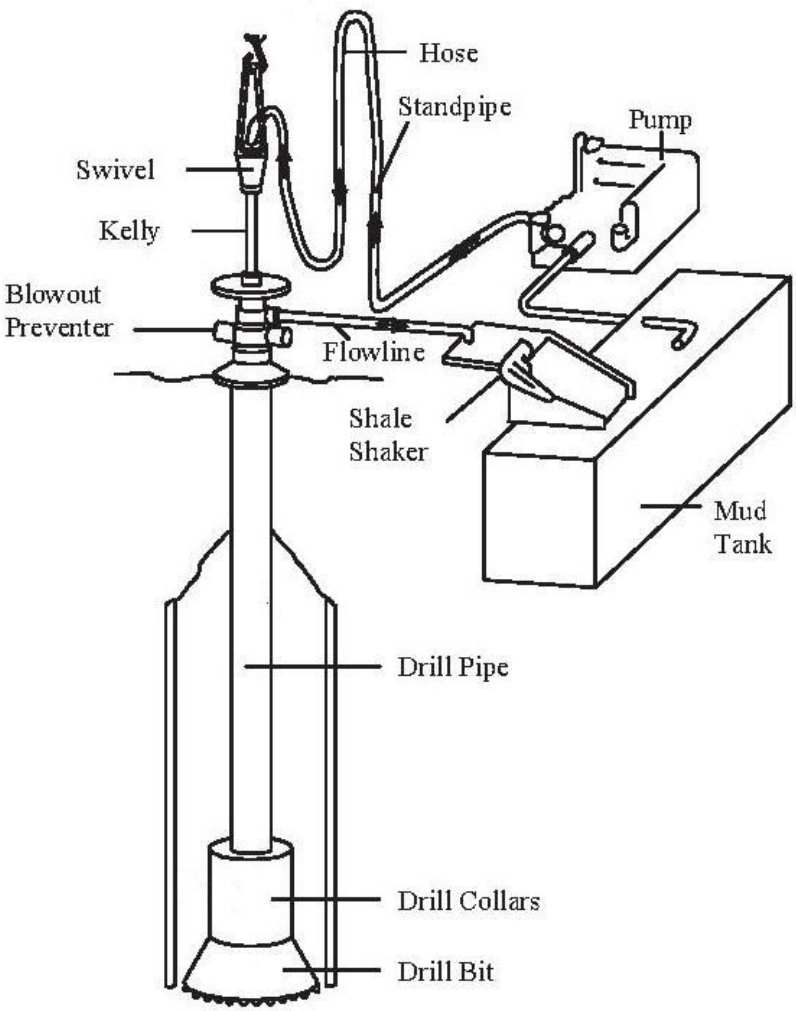

Figure 1.1 : The wellbore hydraulic system (Hussain, 2001).

d) Pressure drop across the bit, which is greatly influenced by the size of nozzles used and the flow rate. For a given flow rate the smaller the nozzles the greater the pressure drop and in turn, greater the nozzle velocity.

The hydraulic system has many effects on a drilling performance and since it is attributed to mud system mostly, the purpose of mud and hydraulics are common to eachother. The optimization of hydraulic system most of the time, ensures the efficiency of a drilling operation. The hydraulic system serves the following functions.

- controlling formation pressures,
- removing drill cuttings from the hole, cleaning the bit,
- suspending drill cuttings when circulation is stopped,

- increase ROP,
- selecting surface equipment such as mud pumps,
- promoting borehole stability,
- allowing real time information to be obtained from the well,
- controling surge pressures,
- reducing swab pressures.

Therefore, it can be stated that a hydraulic system plays an important role in terms of bit optimization, reducing stand pipe pressure (SPP) and frictional pressure losses, and promoting wellbore stability.

1.2 Surge and Swab Pressures While Tripping Opertaion

Tripping pipe or making a round trip is the physical act of pulling the drillstring out of wellbore and then running it back in. This is done by breaking out or disconnecting (when pulling out of hole) every other 2 or 3 joints of drillpipe (stand) at a time and racking them vertically in the derrick. The tripping operations is performed frequently during drilling, for adding a new stand of pipe to reach the target depth, besides this to run the downhole tools for conducting a logging survey, the drillstring is removed at various depths. Considering the problems due to which tripping is also performed, includes fishing trip or retrieval of dropped items and broken strings, but the most typical reason is to replace a worn-out drill bit. When tripping the drill string acts as a large piston moving in the borehole. This movement creates pressures due to friction losses between the moving string and the borehole fluid. Surge and swab pressures, which are generated during drilling operations are very crucial for effective drilling plan and hence downhole pressure management has become important for the industry. Improper estimation of swab and surge pressure, can lead to a number of costly drilling problems, such as lost circulation due to formation fracturing, and fluid influx. The scenario for formation fracturing is illustrated in Figure 1.2, as drillstring is running into hole with high speed, causes excessive surge pressure and fractures the formation. Loss circulation occurs when drilling fluid flows into these fractured zone instead of returning through the annulus, which can results in the reduction of vertical height in the mud column.

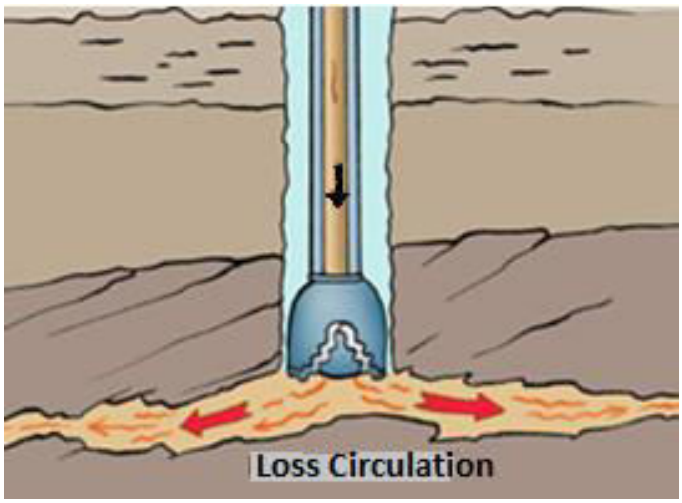

Figure 1.2 : Loss circulation (Halliburton, 2013)

The scenario for fluid influx is shown in Figure 1.3. While pulling drillstring out from the hole, can cause excessive swab pressure, and formation fluid flows into the borehole, results in a well kick. In both scenarios, the worst condition may occur in the form of blowouts.

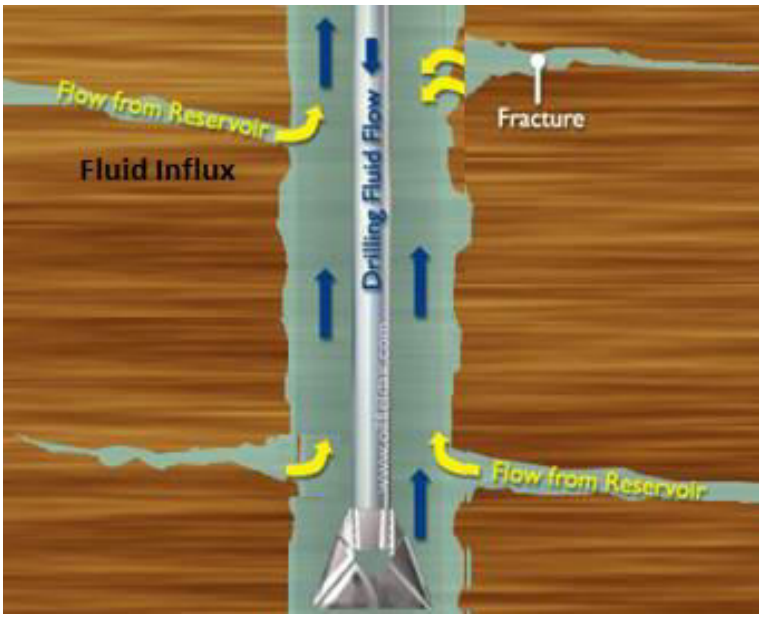

Figure 1.3 : Fluid influx (Halliburton, 2013)

Blowouts often occur during the pipe removal action of a trip as the formation gas (trip gas) enters the hole and lightens the mud column to reduce borehole hydrostatic pressure. Horn (1951) showed that out of 55 blowouts occured in California, 9 gave strong evidence that the reduction in downhole pressure during pipe withdrawal was the cause. Besides these problems the excessive surge and swab pressures may cause hole sloughing, solids bridging and solids filling on bottom. Such wellbore instability

issues are incrementing the non-productive time (NPT) and ultimately rising overall drilling cost. An appropriate estimation of surge pressures is very important in planning drilling operations without having such problems, mainly in wells like slimholes and deepwater wells that exhibit narrow safe pressure window. As pipe moves downward in a hole, the drilling fluid must move upward to evacuate the space being occupied by the volume of moving-in pipe. Likewise, an upward pipe movement requires a downward fluid movement. The flow pattern of the moving fluid can be either laminar or turbulent, depending on the velocity at which the pipe is moving. Figure 1.4 shows the changes in bottomhole pressure in a well while single joint of casing is added to the casing string and lowered into the hole. The causes for the bottomhole pressure peaks in Figure 1.2 are; (a) the casing is lifted from the slips with the effect of pulling out of hole, (b) the pipe string is lowered at maximum velocity, (c) the brake is applied to stop lowering the pipe that caused the bottomhole pressure decrease.

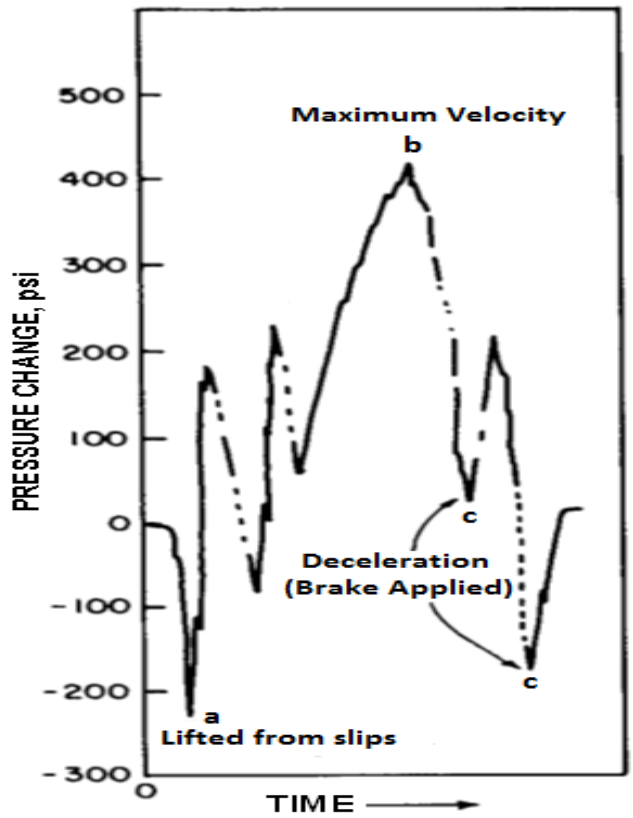

Figure 1.4 : Pressure surges while casing joint is lowered in hole (Bourgoyne, 1991).

In general, the pressure surges caused by inertial effects tend to be less than those caused by viscous drag.

2. LITERATURE REVIEW

Surge and swab pressure is a well known issue in oil industry. Number of studies have been undertaken to understand the surge and swab pressures, dated as early as 1930's. In 1934 pressure surges due to swabbing was detected by Cannon as a potential reason for fluid influx into the wellbore. In 1934, Canon described that hydrostatic pressure changes due to withdrawing drill pipe out of hole. He discussed the factors such as effect of gel strength, effect of mud weigth and viscosity, which resulted in direct proportionality to pressure drop. Model for Bingham Plastic fluid was developed by Burkhardt in 1961 and he also considered the pipe movement. Schuh (1964) presented a model for power law fluids.

In 1951, Goins et al. studied the down hole pressure surges and their effect on loss of circulation. He identified surges caused by running pipe in hole, rapidly opening pumps to start circulation and suggested that these surges may be avoided through slowed rates of pipe movement and slow breaking of circulation.

Burkhardt in 1961 explained wellbore pressure surges produced by pipe movement and made a comparison between the measured surge values and the results predicted by calculation. He correctly predicts the existence and magnitude of various positive and negative peaks due to gel breaking, inertia and viscous drag of the mud. He concluded that while running drill pipe or casing in hole without fill-up devices, the surge due to viscous drag is usually highest.

Mitchell (1988) presented a paper on dynamic surge and swab predictions. He explained that a dynamic model predicts these pressures more accurately than a steady state model, thereby providing better estimates of pressure fluctuations while pipe is tripped. He included the features of (1) longitudinal pipe elasticity and fluid viscous forces to determine pipe displacement; (2) fluid properties that would vary as a function of temperature and pressure; and (3) formation ellasticity and pipe elasticity to determine the response of the borehole. He concluded that in shallow wells, inertial forces and frictional forces seems to be most important, while in deeper wells the compressibilty is important. According to Mitchell, not considering

the effect of fluid compressibility is a conservative assumption, as it predicts a higher flow rates and exhibits higher frictional pressure drops. The surge field tests of Burkhardts and Clark were simulated and to study the importance of dynamic effects, steady state version of surge model was developed and used to compare field data. This showed complete consistency between dynamic and steady state model as shown in Figure 2.1

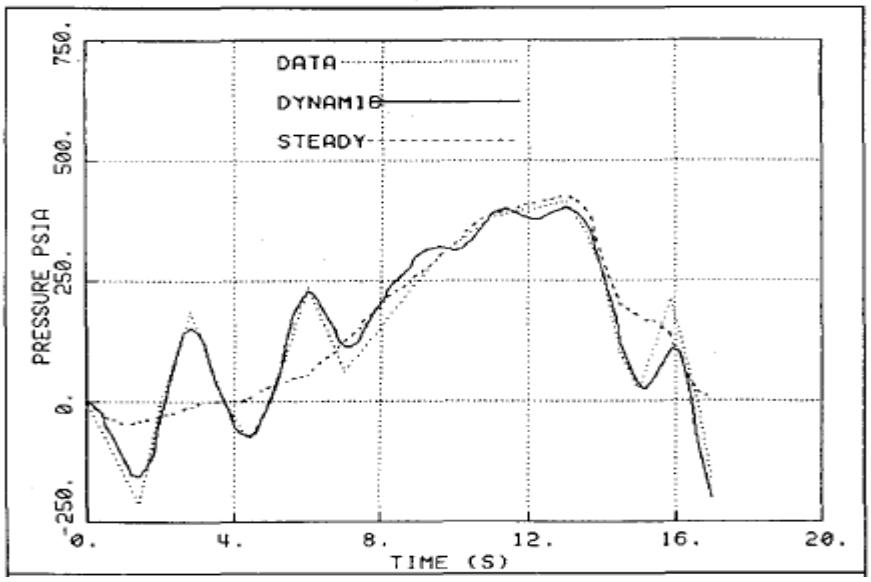

Figure 2.1 : Burkhardt pressure predictions (Mitchell, 1988).

He again used the model for the different test data, taken from Clark and Fontenot's Mississippi well test. The steady flow surge predictions exceed the measured pressures by about 100% as shown in Figure 2.2.

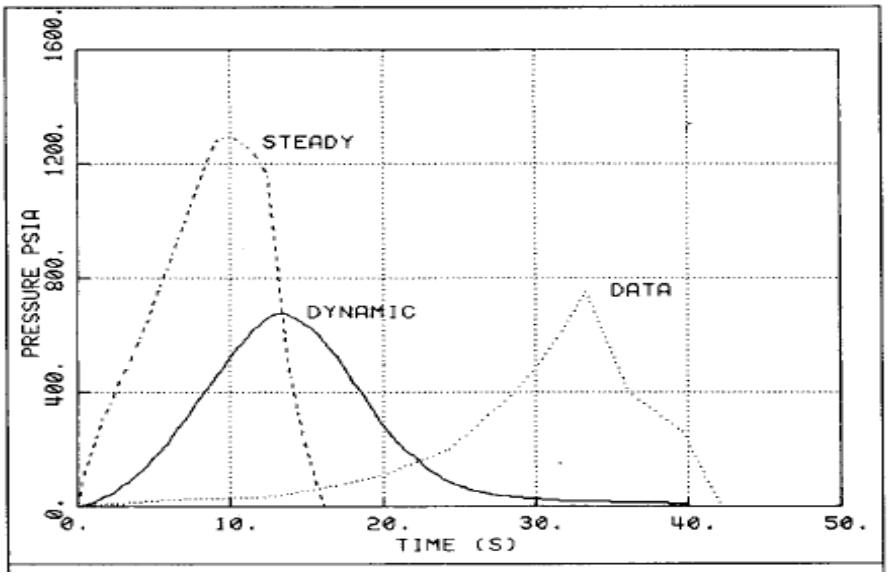

Figure 2.2 : Pressure Predictions, Mississippi Test-1 (Mitchell, 1988).

The dynamic surge model matches the peak pressure measured with in 10% but the measured pressure surges are displaced by about 20 seconds from the predicted surge. For another test conducted in Mississippi well, again he obtained different results for his model. The steady flow surge prediction exceeds the measured pressures by about 50%, as shown in Figure 2.3.

The Mississippi well measurements were quite different from Burkhardt results due to higher well fluid viscosities in Mississippi. The steady flow model overpredicts peak surge pressures.

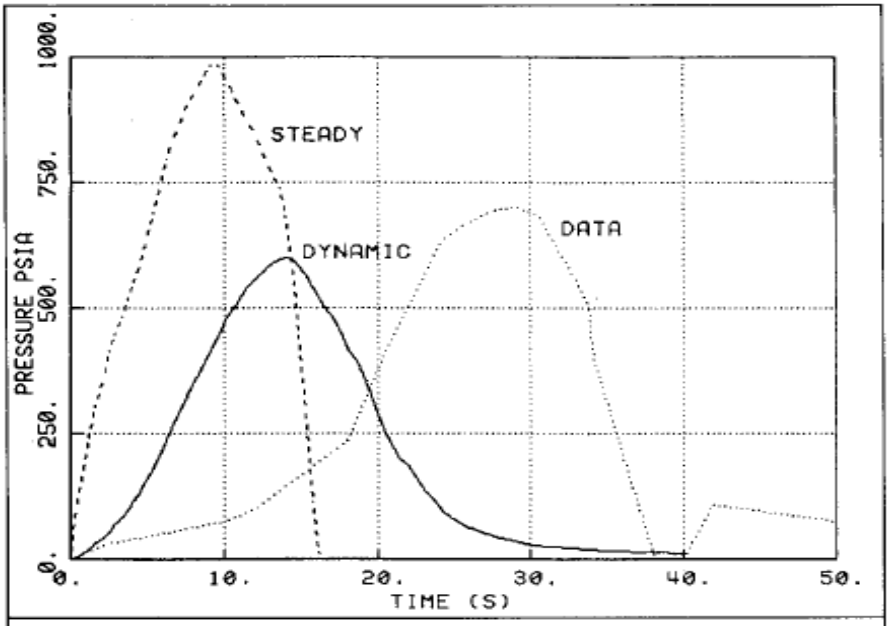

Figure 2.3 : Pressure Predictions, Mississippi Test-2 (Mitchell, 1988).

In 2010, Crespo.F., et al studied surge and swab pressure predictions for yield power law drilling fluids. They showed that the pressure surge depends strongly on drill pipe tripping speed, wellbore geometry, flow regime, fluid rheology and whether pipe is open or closed. Surge and swab pressure is also attributed to different flow phenomena including pipe eccentricity, geometry irregularities, acceleration and dynamic effects.

Merlo et. al. (1995), described an innovative hydraulic computer program developed in Agip, which calculated the rheological parameters of drilling fluid based on viscometer readings, using Newton, Bingham, Power law and Herschel Bulkley rheological models. The program calculated total pressure drop along the well for different depths and also calculated temperature profile of drilling fluid and took into

account the temperature effect on the rheological parameters. A series of circulation test has been monitored in the well A, an ultradeep vertical well located in Po Valley, Italy. The test was carried out at different depths in the 17 ½" and 12 ¼" sections while making a POOH trip, accompanied with circulation. The pressure drops calculated by using the hydraulics computer program are almost accurate compared to the field data, by using the Herschel Bulkley model. The analytical solution described for frictional pressure drop calculations in pipe and annulus using Herschel Bulkley rheological model, has been used in this thesis work to estimate the surge pressures.

3. SCOPE OF THE THESIS

The main objective of this study is to utilize the method presented by Merlo et al. for predicting frictional pressure drops in the wellbore using Herschel-Bulkley model and following standard approach to calculate surge/swab pressure. Within the scope of study the objective is also to compare the results with one of highly used landmark software – Paradigm Sysdrill (Version.10). The effect of pipe velocity or tripping speed (Vp), hole clearance (annular diameter), effect of temperature and effect of fluid density on surge/swab pressure prediction are investigated. The surge pressures are also estimated, using Bingham Plastic model and Power Law model, and compared with the results taken from Herschel Bulkley rheological model. The drilling mud which has been considered for the study is fresh water unweighted sepiolite mud and fresh water weighted sepiolite mud. The reason of using sepiolite mud is that, the study has shown its stability and competency of providing good rheological properties even upto 260°C (Altun et al.,2014). The rheology of sepiolite mud has been taken using both Fann35A viscometer and Fann50SL rheometer at temperatures in the range of 100°F to 450°F, for aging and non-aging conditions respectively to investigate the effect of temperature on surge/swab pressure calculations. In this study, the vertical wellbore condition is used for the calculations and it is assumed that the annulus is concentric, the fluid is incompressible and the steady state conditions are existing.

To the best of knowledge in literature no solution has been published so far for calculating surge/swab pressure using Herschel-Bulkley analytical model for the case, having no drilling fluid circulation (only having drillstring movement). However in the literature, using Herschel-Bulkley analytical model, estimation of stand pipe pressures (SPP) has been done before, while considering drilling fluid circulation at different flow rates.

4. SURGE AND SWAB PRESSURE CALCULATIONS

The main focus of this chapter is to present the brief overview of different fluid analytical models and equations for frictional pressure losses. Specifically Herschel-Bulkley model for calculating surge and swab pressure, caused by the movement of pipe is elaborated.

4.1 Theory of Rheological Models

Fluids can be characterized on the basis of their behaviour based on rheology. Rheology is defined as the deformation of matter, the study of relationship between applied forces (shear stress) at different shear rates. A mathematical model describes the relationship between shear stress and shear rate. These models can be used to calculate friction pressures, swab and surge pressures and slip velocities.

4.1.1 Newtonian model

Shear stress and shear rate can be explained by considering two plates separated with a specific distance having fluid in between. If a force is applied to upper plate while lower plate is stationary, a velocity will be reached that would be function of force. Mathematically, it can be described by Equation 4.1.

$$\frac{F}{A} = \mu \frac{V}{L} \tag{4.1}$$

Where;

F = Force applied to the plate (dyne),

A= Contact area (cm^2),

V= Plate velocity (cm/s),

L= Spacing between plates (cm),

μ= Fluid viscosity (dyne.s/cm^2 or poise).

The left hand term is called the shear stress (τ), while right hand term in the equation is shear rate (γ). The Newtonian model given in Equation 4.2, states that the shear stress is directly proportional to shear rate.

$$\tau = \mu \gamma \quad \textbf{(4.2)}$$

The shear stress and shear rate are analogous to pump pressure and pump rate respectively, in drilling operations.

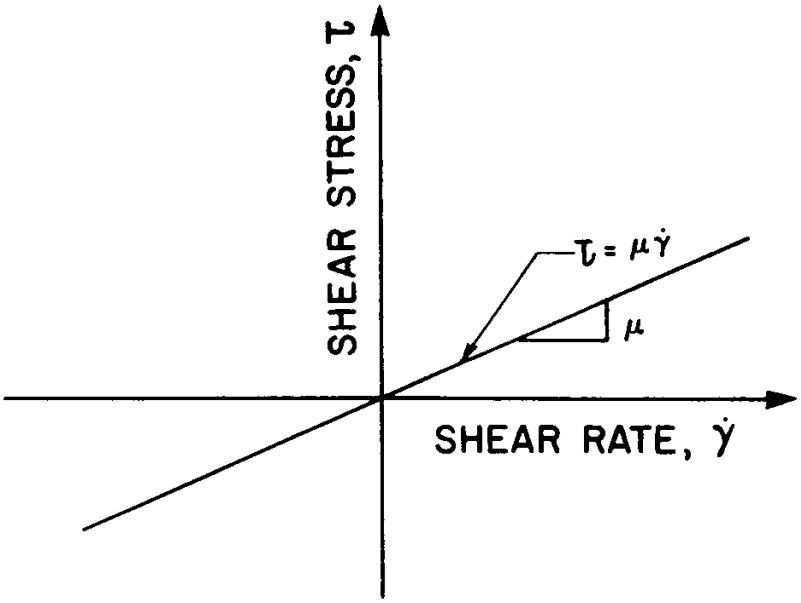

Figure 4.1 : Shear stress vs. shear rate for Newtonian fluid (Bourgoyne, 1991).

The slope in the graph is true or effective viscosity. The fluids with a constant viscosity for all shear rates are called Newtonian. Examples of Newtonian fluids are water, gases and high gravity oils.

4.1.2 Bingham Plastic model

This is a model used to chareacterize fluids that would not flow until the applied shear stress exceeds certain minimum value known as yield stress (τ_y). After this point the stress is directly proportional to the shear rate.

$$\tau = \tau_y + \mu_p \gamma \quad \textbf{(4.3)}$$

Where;

τ = Shear stress, Pa or lb.f/sq.ft

τ_y = Yield point, Pa or lb.f/sq.ft

μ_p = Plastic viscosity, Pa.s or cP

γ = Shear rate, s^{-1}

Under low shear stress, Bingham fluid acts as a rigid body and under high shear stress acts as a viscous fluid. In the figure below, the line does not start at the origin but after the yield stress, where the shear rate is zero and the slope of line is the plastic viscosity.

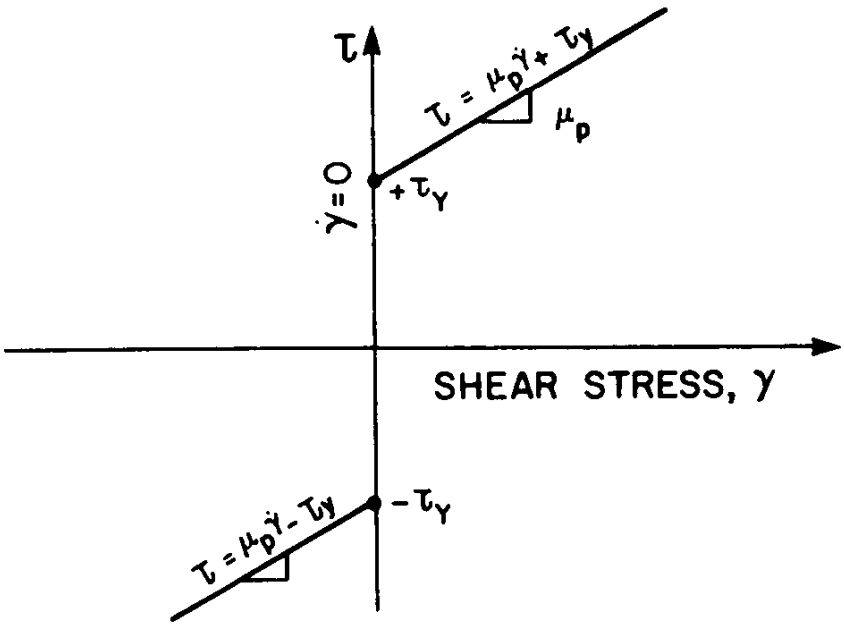

Figure 4.2 : Shear stress vs. shear rate for Bingham plastic fluid (Bourgoyne, 1991).

The equations for calculating frictional pressure losses are explained in Bourgoyne et al., (1991), here only equations are given.

<u>For pressure losses inside pipe</u>

$$\frac{dp_f}{d_L} = \frac{\mu_p \ \overline{v}}{1500d^2} + \frac{\tau_y}{225d} \tag{4.4}$$

$$\frac{dp_f}{d_L} = \frac{\rho^{0.75} \ \overline{v}^{1.75} \ \mu_p \ ^{0.25}}{1800d^{1.25}} \tag{4.5}$$

Eq.4.4 is for laminar flow and Eq.4.5 is for turbulent flow respectively.

<u>For pressure losses inside annulus</u>

$$\frac{dp_f}{d_L} = \frac{\mu_p \ \overline{v}}{1000(d_2 - d_1)^2} + \frac{\tau_y}{200(d_2 - d_1)} \quad \textbf{(4.6)}$$

$$\frac{dp_f}{d_L} = \frac{\rho^{0.75} \ \overline{v}^{1.75} \ \mu_p^{\ 0.25}}{1396(d_2 - d_1)^{1.25}} \quad \textbf{(4.7)}$$

Eq. 4.6 is for laminar flow and Eq. 4.7 is for turbulent flow respectively. Note that the parameters in these equations are in customary or field units.

4.1.3 Power Law model

Power law fluids also known as Ostwald-de Waele fluid model. This is a nonlinear relationship between shear stress and shear rate. The mathematical form is given as,

$$\tau = K(\gamma)^n \quad \textbf{(4.8)}$$

K = Consistency index,

n = Power law exponent or flow behaviour index.

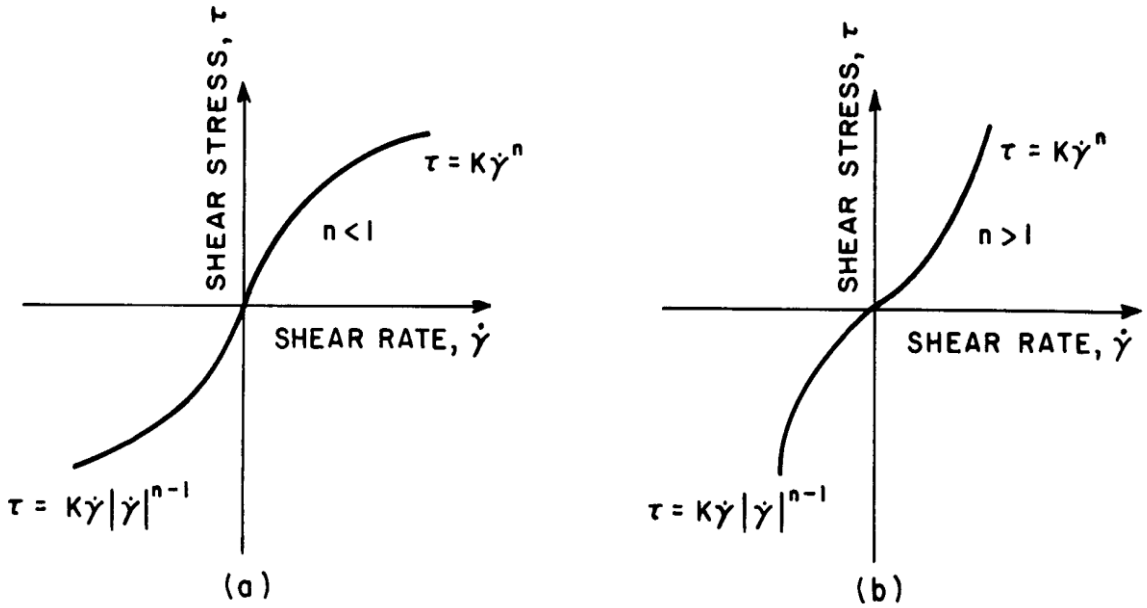

Figure 4.3 : Shear stress vs shear rate for Power Law fluid: (a) pseudoplastic fluid, and (b) dilatant fluid (Bourgoyne, 1991).

The power law model requires two parameters, K and n, for fluid characterization. If (n<1) it represents pseudoplastic fluid; if (n=1), Newtonian fluid; if (n>1), then dilatant fluid respectively.

The behaviour in Figure 4.3 is curved unlike the Newtonian fluid. If the slope, which is a measure of apparent viscosity, is taken at each point on the curve in, (a) the slope is decreasing for increasing shear rate, hence it is termed as pseudoplastic and the slope in (b) is increasing with increasing shear rate, hence it is termed as dilatant. The equations for calculating frictional pressure losses are as below.

<u>For pressure losses inside pipe</u>

$$\frac{dp_f}{d_L} = \frac{K \ \overline{v}^n \ \left(\frac{3 + 1/n}{0.0416}\right)^n}{144000 \ d^{1+n}} \tag{4.9}$$

$$\frac{dp_f}{d_L} = \frac{f \ \rho \ \overline{v}^2}{25.8 \ d} \tag{4.10}$$

Eq. 4.9 is for laminar flow and Eq. 4.10 is for turbulent flow respectively.

<u>For pressure losses inside annulus</u>

$$\frac{dp_f}{d_L} = \frac{K \ \overline{v}^n \ \left(\frac{2 + 1/n}{0.0208}\right)^n}{144000 \ (d_2 - d_1)^{1+n}} \tag{4.11}$$

$$\frac{dp_f}{d_L} = \frac{f \ \rho \ \overline{v}^2}{21.1 \ (d_2 - d_1)} \tag{4.12}$$

Eq. 4.11 is for laminar flow and Eq. 4.12 is for turbulent flow respectively.

4.2 Herschel-Bulkley Model

Herschel-Bulkley model is also known as Yield Power law model and it is a combination of Bingham Plastic and Power law models. It is a three parameter model includes yield stress, consistency index and flow behavior index. Mathematical form of the models is;

$$\tau = \tau_y + K\gamma^n \tag{4.13}$$

This equation can be reduced to Power law model if yield stress, (τ_y) is set to zero.

$$\tau = K(\gamma)^n \tag{4.14}$$

If flow behavior index, (n) is taken as one, then Eq. 4.13 reduces to Bingham plastic model, and consistency index, (K) becomes plastic viscosity.

If flow behavior index, (n) is taken as one, and yield stress, (τ_y) sets to zero then Eq.4.13 reduces to Newtonian fluid model and consistency index becomes apparent viscosity.

$$\tau = \mu_a \gamma \tag{4.15}$$

In Figure 4.4, the graphical comparison of above mentioned rheological models is given.

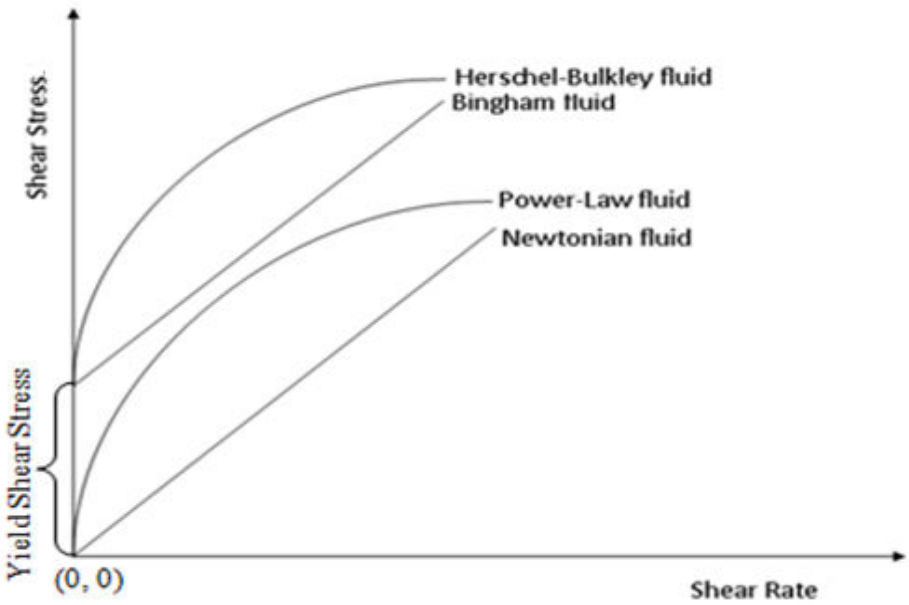

Figure 4.4 : Comparision of rheological models. (Skalle, 2012).

4.2.1 Equations for frictional pressure loss calculation

For calculating frictional pressure losses, the most important Herschel-Bulkley equations both for pipe interior and annulus are described here.

Reynolds number is used to determine flow regime. After determining the flow regime the appropriate equations will be used to predict pressure losses.

$$R_e = \frac{2\rho Q}{\mu \pi R} \tag{4.16}$$

Equation 4.16 shows a generalized Reynolds number. In Herschel-Bulkley model, it is needed to determine equivalent Reynolds number, which is defined as follows,

$$Re_{eq} = Cc * Re \tag{4.17}$$

Here C_c is correction factor and is defined as follows,

$$C_c = 1 - \frac{1}{2n+1}\left[\frac{\tau_o}{\tau_o + k\left\{\frac{(3n+1)Q}{n\pi R^3}\right\}^n}\right] \tag{4.18}$$

As it can be seen from Equation 4.16, for Reynolds number calculations, viscosity is needed. Formula below shows how to calculate viscosity;

$$\mu = \frac{\tau_0 + \mathrm{K}\left[\left(\frac{3n+1}{n\mathrm{Cc}}\right)\left(\frac{\mathrm{Q}}{\pi \mathrm{R}^3}\right)\right]^n}{\left(\frac{3n+1}{n\mathrm{Cc}}\right)\left(\frac{\mathrm{Q}}{\pi \mathrm{R}^3}\right)} \tag{4.19}$$

Flow rate can be written as cross sectional area multiplied by velocity of fluid passing through that cross-sectional area;

$$Q = (\pi R^2)V_p \tag{4.20}$$

After making substitutions for flow rate and viscosity, equivalent Reynolds number becomes as follow,

$$Re_{eq} = 2\left(\frac{3n+1}{n}\right)\left(\frac{\rho V_p^{(2-n)} R^n}{\tau_0\left(\frac{R}{V_p}\right)^n + k\left(\frac{3n+1}{nCc}\right)^n}\right) \tag{4.21}$$

To decide whether flow is laminar or turbulent, equivalent Reynolds number should be compared with critical Reynolds number which is described as follows;

$$Re_{eqcr} = (Cc * Re)_{cr} = \left[\frac{4(3n+1)}{ny}\right]^{\left(\frac{1}{1-\mathrm{z}}\right)} \tag{4.22}$$

where,

$$y = \frac{\log(n) + 3.93}{50} \tag{4.23}$$

and,

$$z = \frac{1.75 - \log(n)}{7} \quad \textbf{(4.24)}$$

As a criteria the following should be taken into account;

If $Re_{eq} \leq Re_{eqcr}$ the flow is considered laminar, but if $Re_{eq} > Re_{eqcr}$ then the flow is considered turbulent.

<u>Calculations in pipe</u>

Now consider pressure drop calculations for laminar flow. It is calculated using Fanning expression:

$$\Delta p = f\rho \frac{Q^2}{\pi^2 \ R^5} L \quad \textbf{(4.25)}$$

While the friction factor in the equation above is determined by the following equation.

$$f = \frac{4}{R_{\text{e eq}}} * \left(\frac{3n+1}{n}\right) \quad \textbf{(4.26)}$$

Concentrate on the pressure drop equation for turbulent flow;

$$\Delta p = f\rho \frac{Q^2}{\pi^2 R^5} L \quad \textbf{(4.27)}$$

while the friction factor in the equation above is determined by the following equation ;

$$f = y(Cc * Re)^{-z} \quad \textbf{(4.28)}$$

where y and z are the coefficients which are described above.

<u>Calculations in annuli</u>

Pressure drop calculations for pipe flow regime should be determined before going into calculations. To determine flow regime equivalent Reynolds number must be calculated and compared with critical Reynolds number. Equivalent Reynolds number can be calculated as follow;

$$Re_{eq} = Ca * Re \tag{4.29}$$

where

$$Ca = 1 - \frac{1}{n+1}\left[\frac{\tau_o}{\tau_o + k\left\{\left(\frac{2(2n+1)}{n(R_2 - R_1)}\right)\left(\frac{Q}{\pi({R_2}^2 - {R_1}^2)}\right)\right\}^n}\right] \tag{4.30}$$

$$\mathrm{Re} = \frac{2\rho \mathrm{Q}}{\mu\pi(\mathrm{R}_1 + \mathrm{R}_2)} \tag{4.31}$$

Viscosity and flow rate is required for Reynolds number calculation. Viscosity and flow rate calculation formulae are provided in below equations;

$$\mu = \frac{\tau_o + k\left[\left\{\frac{2(2n+1)}{n(R_2 - R_1)}\right\}\left\{\frac{Q}{\pi\, Ca\, ({R_2}^2 - {R_1}^2)}\right\}\right]^n}{\left\{\frac{2(2n+1)}{n(R_2 - R_1)}\right\}\left\{\frac{Q}{\pi\, Ca\, ({R_2}^2 - {R_1}^2)}\right\}} \tag{4.32}$$

$$Q = \pi(R_2^2 - R_1^2)V_a \tag{4.33}$$

After substituting, we obtained the following equation,

$$Re_{eq} = \left(4\frac{2n+1}{n}\right)\frac{\rho V_a^{(2-n)}(R_2 - R_1)^n}{\tau_0\left(\frac{R_2 - R_1}{VV_a}\right)^n + k\left(2\frac{2n+1}{nCa}\right)^n} \tag{4.34}$$

Critical Reynolds number is define as,

$$Re_{eqcr} = (Ca * Re)_{cr} = \left[\frac{8(2n+1)}{ny}\right]^{\left(\frac{1}{1-z}\right)} \tag{4.35}$$

Where y and z are same as defined in Eq: 4.23 and Eq: 4.24, respectively.

As mentioned above, for flow regime determination equivalent Reynolds must be compared with critical Reynolds number. If $Re_{eq} \leq Re_{eqcr}$ the flow is considered as laminar, but if $Re_{eq} > Re_{eqcr}$, then the flow is considered as turbulent. Now consider frictional pressure loss equations. For laminar flow frictional pressure loss can be calculated by using the following equation;

$$\Delta p = f\rho\, \frac{Q^2}{\pi^2\ (R_2 - R_1)({R_2}^2 - {R_1}^2)^2}\, L \tag{4.36}$$

Where f is dimensionless friction factor and calculated as follows;

$$f = \frac{8}{R_{e\,eq}} * \left(\frac{2n+1}{n}\right) \quad \textbf{(4.37)}$$

Now combine friction factor and Reynolds number with frictional pressure loss;

$$\Delta p = \frac{2LK}{(R_2 - R_1)}\left[\frac{\tau_0}{k} + \left[\left(\frac{2(2n+1)}{nCa(R_2 - R_1)}\right)\left(\frac{Q}{\pi(R_2^2 - R_1^2)}\right)\right]^n\right] \quad \textbf{(4.38)}$$

If the flow regime is turbulent, the frictional pressure loss is calculated by using the formula below;

$$\Delta p = f\rho \frac{Q^2}{\pi^2 \ (R_2 - R_1)({R_2}^2 - {R_1}^2)^2} L \quad \textbf{(4.39)}$$

Where f is dimensionless friction factor and calculated as follows;

$$f = y(Ca * Re)^{-z} \quad \textbf{(4.40)}$$

Where *y* and *z* are the same coefficients defined in Eq:4.23, and Eq:4.24

4.3 Surge and Swab Calculation Approach

A simplified technique for computing surge pressures was presented by Burkhardt, which is based on the use of effective fluid velocity in the annular flow equations and using an effective mean annular velocity, which is comprised of mud clinging constant (K) term. To determine the correct surge and swab pressure, the value of annular fractional flow rate (f_a) must be chosen such that the sum of frictional pressure losses through all sections of the annulus is equal to the sum of frictional pressure losses through all sections of the drillstring interior. The annular fractional flow rate (f_a) is the ratio of flow rate in the annulus to the total flow rate at the bottom of the drillstring.

$$f_a = \frac{q_a}{q_t} \quad \textbf{(4.41)}$$

Where q_t is the summation of flow rates between the pipe interior, q_p and well annulus q_a ,

$$q_t = q_a + q_p \quad \textbf{(4.42)}$$

For the open pipe condition, the problem is to find how the flow is splitting between pipe and annulus, so that the pressures for both pipe and annulus match each other at

the bit. It is a kind of iterative process, which can be done using any computer program like MS Excel. Simple strategy for solving this is mentioned below:

1) Calculate annular pressures with all flow in the annulus. Then check pressures at the bit; annular pressures will be lower because of fluid friction.
2) Calculate all pressures with all flow inside the pipe. Then check pressures at the bit.
3) Calculate a division of flow between the pipe and annulus that will equalize the pressures at the bit.
4) Repeat step 3 until the two pressures match eachother within an acceptable tolerance (i.e. 1 psi or 0.06 bar).

The steps to estimate the surge pressures are given in the flow diagram in Figure 4.5.

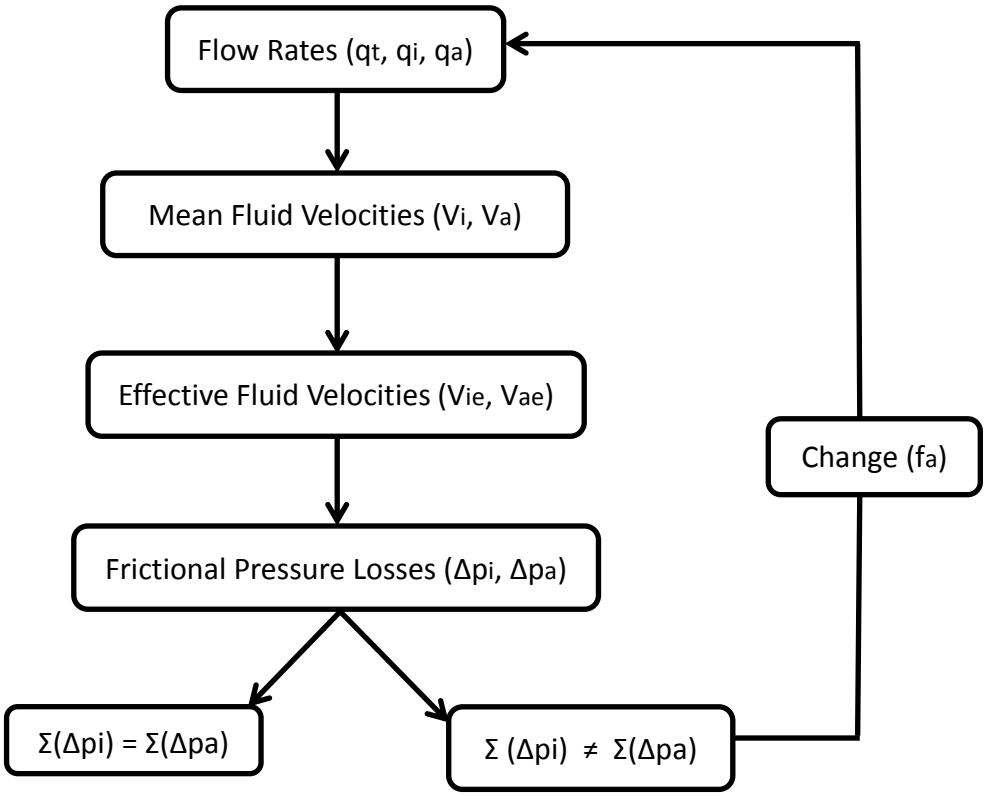

Figure 4.5 : Flow diagram for swab calculations.

When total pressure losses in the annulus become equal to the total pressure losses inside the pipe section, true surge pressure is obtained. If the flowrate in annulus is in a different direction than the flowrate in the pipe interior,value of f_a greater than one or less than zero is possible. Values of f_a which are greater than one tend to occur

when internal area is very small in comparison to the annular area. On the other hand values of f_a which are negative, tend to occur when the annular area is very small in comparison to the internal area.

The equations used to estimate surge pressures, using Herschel Bulkley analytical model are summarized in Table 4.1.

4.4 Paradigm Sysdrill Overview

Paradigm Sysdrill (V.10) provides a comprehensive single application for well planning, survey management and drilling engineering analysis. It allows companies to enhance well planning accuracy, reduce drilling risk and uncertainity, quantify wellbore positioning and improve drilling safety. This software comprises of two main modules that are (1) Sysdrill well planning and survey management and (2) Sysdrill drilling engineering. The flow diagram given in Figure 4.6, describes the functions, that Sysdrill drilling engineering module can perform.

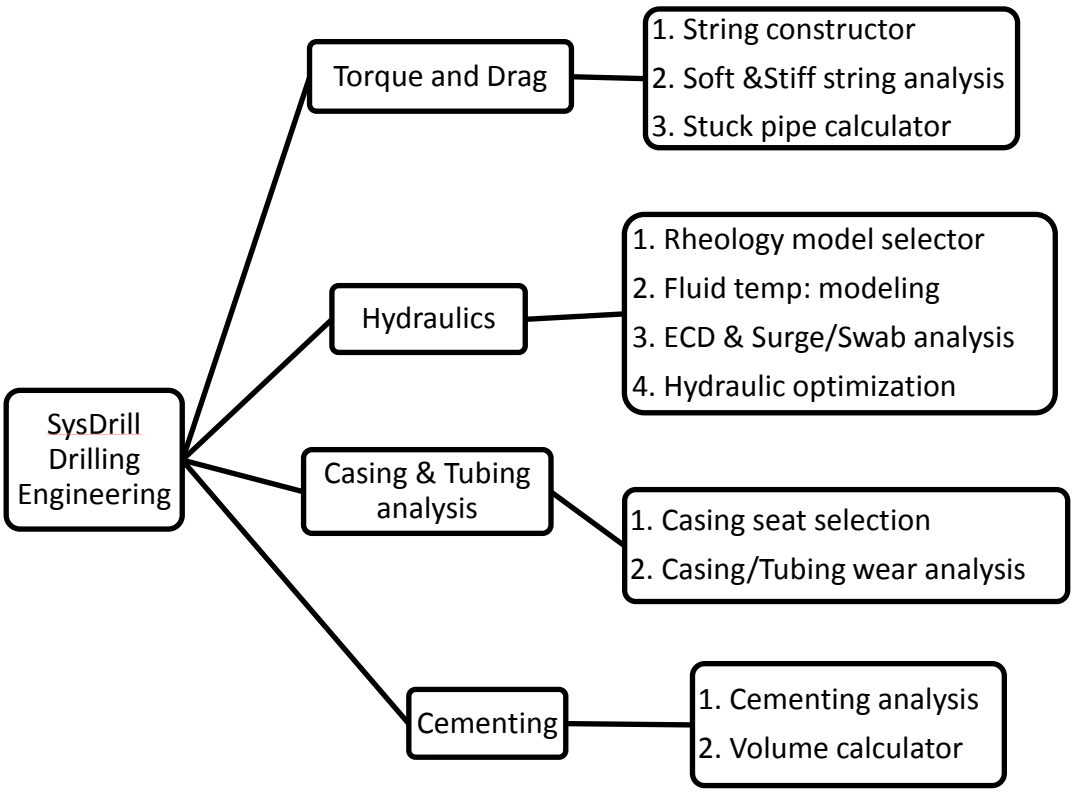

Figure 4.6 : Sysdrill drilling engineering functions (Paradigm).

Hydraulics Analysis

The hydraulics calculation involves hydraulic analysis of a string within a particular hole section. The editor allows efficient definition of inputs, execution of calculations and analysis of results. Major functions that can be performed in this tab are as follows,

- Multiple calculation options, including pump pressure, flow rate, bit total flow area (TFA) and % bit pressure loss.
- Calculation may be run as a static depth analysis or over a depth interval range.
- Visualise fluid density, pressure and velocity against critical limits.
- Pass/Fail summary allows fast identification of specific issues.
- Calculate cuttings transport ratio throughout the annulus.
- Surge and swab, ESD, flow range, BHHP & JIF and fluid volume calculators are also available within the *hydraulics* calculation window.
- Maximum run and pull speeds of the drill string can be calculated with desired safety margin.
- Support for both simple and complex fluid rheology definitions.
- Complex fluid definitions are made within a dedicated *fluid builder* interface which allows description of a fluid's rheology and density behaviour with varied pressure and temperature.
- Fluids and constituent fluid materials may be saved to *catalogue* for re-use.
- Modelling of managed pressure drilling scenerios.

Table 4.1 : Frictional pressure loss equations for Herschel Bulkley model.

	Pipe	Annulus
Turbulence Criteria	i. $Re_{eq} = Cc * Re$ $C_c = 1 - \frac{1}{2n+1}\left[\frac{\tau_o}{\tau_o + k\left\{\frac{(3n+1)Q}{n\pi R^3}\right\}^n}\right]$ $\mathrm{Re} = \frac{2\rho Q}{\mu\pi R}$ Where; $\mu = \frac{\tau_0 + k\left[\left(\frac{3n+1}{nCc}\right)\left(\frac{Q}{\pi R^3}\right)\right]^n}{\left(\frac{3n+1}{nCc}\right)\left(\frac{Q}{\pi R^3}\right)}$ $Q = (\pi R^2)V_p$ ii) $Re_{eqcr} = (Cc * Re)_{cr}$ or $= \left[\frac{4(3n+1)}{ny}\right]^{\left(\frac{1}{1-z}\right)}$	i. $Re_{eq} = Ca * Re$ $Ca = 1 - \frac{1}{n+1}\left[\frac{\tau_o}{\tau_o + k\left\{\left(\frac{2(2n+1)}{n(R_2 - R_1)}\right)\left(\frac{Q}{\pi({R_2}^2 - {R_1}^2)}\right)\right\}^n}\right]$ $\mathrm{Re} = \frac{2\rho Q}{\mu\pi(R_1 + R_2)}$ Where; $\mu = \frac{\tau_o + k\left[\left\{\frac{2(2n+1)}{n(R_2 - R_1)}\right\}\left\{\frac{Q}{\pi\, Ca\, ({R_2}^2 - {R_1}^2)}\right\}\right]^n}{\left\{\frac{2(2n+1)}{n(R_2 - R_1)}\right\}\left\{\frac{Q}{\pi\, Ca\, ({R_2}^2 - {R_1}^2)}\right\}}$ $Q = \pi(R_2^2 - R_1^2)V_a$ ii) $Re_{eqcr} = (Ca * Re)_{cr}$ or $= \left[\frac{8(2n+1)}{ny}\right]^{\left(\frac{1}{1-z}\right)}$
	$y = \frac{\log(n)+3.93}{50}$ $z = \frac{1.75-\log(n)}{7}$ For $\mathrm{Re}_{eq} \leq \mathrm{Re}_{eqcr}$ the flow is laminar For $\mathrm{Re}_{eq} > \mathrm{Re}_{eqcr}$ the flow is turbulent	
Laminar Flow	$\Delta p = f\rho\, \frac{Q^2}{\pi^2\, R^5}\, L$ Where; $f = \frac{4}{R_{e\,eq}} * \left(\frac{3n+1}{n}\right)$	$\Delta p = f\rho\, \frac{Q^2}{\pi^2\, (R_2 - R_1)({R_2}^2 - {R_1}^2)^2}\, L$ Where; $f = \frac{8}{R_{e\,eq}} * \left(\frac{2n+1}{n}\right)$
Turbulent Flow	$\Delta p = f\rho\, \frac{Q^2}{\pi^2\, R^5}\, L$ Where; $f = y(Cc * Re)^{-z}$	$\Delta p = f\rho\, \frac{Q^2}{\pi^2\, (R_2 - R_1)({R_2}^2 - {R_1}^2)^2}\, L$ Where; $f = y(Ca * Re)^{-z}$

5. APPLICATION

In this chapter the steps mentioned in previous chapter for calculating surge pressure for Herschel-Bulkley model is implied in a given wellbore condition. The analytical results are compared with the Sysdrill solution, furthermore sensitivity analysis is carried out for better understanding of the important factors effecting these pressures.

5.1 Herschel-Bulkley Analytical Solution

Well configuration:

Table 5.1: Well specifications

Parameter		In field units	In SI units
Hole diameter		7.875 in	0.2 m
Drillstring length		15000 ft	4572 m
Drillpipe	Length	14300 ft	4358.64 m
	OD	4.5 in	0.1143 m
	ID	3.826 in	0.0971 m
Drillcollar	length	700 ft	213.36 m
	OD	6.25 in	0.158 m
	ID	2.75 in	0.0698 m
Bit	Three nozzles	11/32 in	0.008731 m
	Discharge area	0.2784 sq.in	0.00018 sq.m
	Discharge coefficient	95 % or 0.95	

Drill string is moving through a 10 lb/gal (1198.2 kg/m^3), density of drilling fluid at speed of 4 ft/s (1.219 m/s).

Table 5.2: Fann35A viscometer readings for UWSM at 150°F (UWSM150).

RPM	Dial Reading
600	70
300	44
200	35
100	23
6	5
3	4

After inserting these readings to Sysdrill's Fluid Builder option in hydraluics section, the rheological parametrs for Herschel- Bulkley came out to be.

n = 0.66 , K =349.68 (mPa.s) , τ_y = 1 (Pa)

Model Graphs | Fann Data

	RPM [rpm]	Shear Stress [Pa]	Shear Rate [/sec]	Measured Angle [deg]	Bingham Plastic Shear Stress [Pa]	% [%]	Herschel Bulkley Shear Stress [Pa]	% [%]	Power Law Shear Stress [Pa]
1	600.00	35.78	1021.65	70.00	37.71	5.41	35.66	-0.33	33.11
2	300.00	22.49	510.82	44.00	20.93	-6.93	22.89	1.77	22.74
3	200.00	17.89	340.55	35.00	15.33	-14.28	17.73	-0.91	18.26
4	100.00	11.76	170.27	23.00	9.74	-17.15	11.56	-1.63	12.54
5	6.00	2.56	10.22	5.00	4.48	75.32	2.64	3.24	2.73
6	3.00	2.04	5.11	4.00	4.31	110.94	2.04	-0.40	1.88

Fluid Model Parameters

Power Law	n	0.66	
Bingham Plastic	K	349.68	mPa.s
Robertson Stiff	Ty	1.00	Pa
Herschel Bulkley			

Figure 5.1 : Herschel-Bulkley rheological parameters.

The nomenclature shown in Figure 5.2 has been taken in the solution of this problem. For simplicity, the effect of the outer shape of the bit and effect of tool joints are assumed to be negligible and are ignored. In addition, it is assumed that the hole is kept full and fluid level in the pipe and annulus are maintained equal approximately.

<u>Calculation for pipe interior</u>

The total flow rate near the bottom of drill string is given as,

$$q_t = v_p \left[\frac{\pi}{4} {d_1}^2 - A_j\right] \tag{5.1}$$

$$q_t = 1.2192 \left[\frac{\pi}{4} 0.1587^2 - 0.00018\right] = 0.02391\ m^3/sec$$

The flow rate through the bit jets is given by,

$$q_{(p)1} = (1 - f_a)\,(q_t) \tag{5.2}$$

If f_a is taken as 0.5 for initial guess then,

$$q_{(p)1} = (1 - 0.5)\,(0.02391) = 0.011956\ m^3/sec$$

The flow rates in drill collar and drill pipe interior are given by Eq: 5.3.

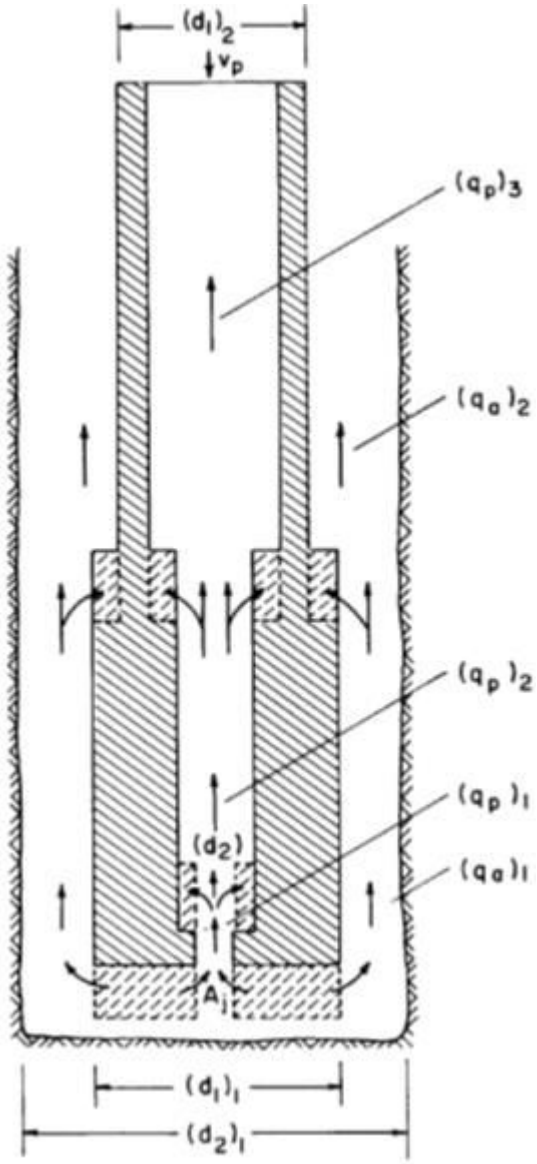

Figure 5.2 : Hydraulic representation of lower part of drill string (Bourgoyne, 1991).

$$\left(q_p\right)_i = \left(q_p\right)_{i-1} - \frac{\pi}{4} v_p \left[(d_i)^2 - (d_{i-1})^2 \right] \quad \textbf{(5.3)}$$

$$q_{(p)\,2} = (0.011956) - 1.2192 \left[\frac{\pi}{4} 0.06985^2 - 0.00018\right]$$
$$= 0.007504\ m^3/sec$$

$$q_{(p)\,3} = (0.007504) - 1.2192 \left[\frac{\pi}{4} 0.09718^2 - \frac{\pi}{4} 0.06985^2\right]$$
$$= 0.003132\ m^3/sec$$

The mean fluid velocity (with respect to an observer at the surface) through bit jets is given by,

$$(v_i\ )_1 = \frac{(q_p\ )_1}{(A_p\ )_1} \quad \textbf{(5.4)}$$

$$v_{(i)1} = \frac{0.011956}{0.00018} = 66.568\ m/sec$$

Similarly, fluid velocity in the drill collar and drill pipe interior is,

$$v_{(i)2} = \frac{0.007504}{\frac{\pi}{4}\ 0.06985^2} = 1.958\ m/sec$$

$$v_{(i)3} = \frac{0.003132}{\frac{\pi}{4}\ 0.09718^2} = 0.422\ m/sec$$

The effective fluid velocity (with respect to the nozzle wall) through the bit jets is given by,

$$v_{(ie)1} = v_{(i)1} + v_p = 66.568 + 1.2192 = 67.787\ m/sec \quad \textbf{(5.5)}$$

Similarly, effective fluid velocity (with respect to the pipe wall) in drill collar and drill pipe is given as,

$$v_{(ie)2} = v_{(i)2} + v_p = 1.958 + 1.2192 = 3.177\ m/sec$$

$$v_{(ie)3} = v_{(i)3} + v_p = 0.422 + 1.2192 = 1.641\ m/sec$$

The pressure loss through the bit jets is calculated through rearrangement, use of $(v_{ie})_1$ in place of v_n with the following equation and using unit conversion factors.

$$v_n = C_d \sqrt{\frac{\Delta p_b}{8.074 * 10^{-4}\ \rho}} \quad \textbf{(5.6)}$$

$$\Delta p_b = \frac{v_{(ie)1}{}^2 * 7.2 * 10^{-5} * \rho}{C_d{}^2} = \frac{67.787^2 * 7.2 * 10^{-5} * 1198.2}{0.95^2}$$
$$= 439.8212 \text{ psi}$$

Using Eq:4.20, flow rates across drillcollar and drillpipe are calculated, and effective fluid velocities are considered.

Q_{dc}= 0.012175 m^3/sec and Q_{dp}= 0.0121 m^3/sec

Find correction coefficient for both sections, using Eq: 4.18

$(C_c)_{dc}$ = 0.9779 and $(C_c)_{dp}$ = 0.9595

Newtonian viscosity is calculated using Eq: 4.19

μ_{dc}= 0.04722 (Pa.sec) and μ_{dp} =0.06868 (Pa.sec)

$(Re)_{dc}$= 5634.27 and $(Re)_{dp}$=2784.28 using Eq: 4.16

$(Re_{eq})_{dc}$= 5510.169 and $(Re_{eq})_{dp}$= 2671.66 using Eq: 4.17

Using Eq: 4.22, Critical equivalent Reynolds numbers both for drillcollar and drillpipe are calculated, which came out to be same, because it is only dependent to the fluid parameter (n). The terms *y* and *z* are defined by Eq:4.23 and Eq:4.24, the values are 0.07499 and 0.2757 respectively.

Re_{eqcr}= 1943.89

In both sections flow came out to be turbulent, after applying flow criteria, so using Eq: 4.28 fanning friction factor (*f*) and then using Eq: 4.27 pressure loss is calculated.

$(f)_{dc}$= 0.00697 and $(\Delta p)_{dc}$= 5.1563 bar (75.5404 psi)

$(f)_{dp}$= 0.00851 and $(\Delta p)_{dp}$= 24.6728 bar (361.4571 psi)

<u>Calculation for annular section</u>

Now the flow rates, velocities, effective velocities and frictional pressure losses in the annulus are determined using similar procedure as used for pipe interior.

Flow rate in section one i.e. drill collar is calculated with following equation,

$$(q_a)_1 = f_a\,(q_t)_1 \qquad \textbf{(5.7)}$$

$$(q_a)_1 = 0.5 * 0.02391 = 0.01196\, m^3/sec$$

Flow rate in section two; i.e. drill pipe is calculated as,

$$(q_a)_i = (q_a)_{i-1} - \frac{\pi}{4}\, v_p\left[(d_1)^2{}_{i-1} - (d_1)^2{}_i\right] \qquad \textbf{(5.8)}$$

$$(q_a\ )_2 = 0.01196 - \frac{\pi}{4} * 1.2192\ (0.15875^2 - 0.1143^2) = 0.00033\ m^3/sec$$

The mean annular fluid velocity (with respect to an observer at the surface) is given as,

$$(v_a\ )_1 = \frac{(q_a\ )_1}{(A_a\ )_1} \qquad \textbf{(5.9)}$$

$$(v_a\ )_1 = \frac{0.01196}{\frac{\pi}{4}(0.20003^2 - 0.15875^2)} = 1.028\ m/sec$$

$$(v_a\ )_2 = \frac{0.00033}{\frac{\pi}{4}(0.20003^2 - 0.1143^2)} = 0.016\ m/sec$$

The effective annular fluid velocity is given by using mud clinging constant (K), which is calculated with Figure A.1.

$$(v_{ae})_1 = (v_a)_1 + Kv_p = \begin{cases} for\ laminar \\ for\ Turbulent \end{cases} \qquad \textbf{(5.10)}$$

$$(v_{ae})_1 = \begin{cases} 1.028 + (0.462 * 1.2192) = 1.591\ \ laminar \\ 1.028 + (0.499 * 1.2192) = 1.637\ \ Turbulent \end{cases}$$

$$(v_{ae})_2 = \begin{cases} 0.016 + (0.409 * 1.2192) = 0.514\ \ laminar \\ 0.016 + (0.491 * 1.2192) = 0.6138\ \ Turbulent \end{cases}$$

As there are two conditions in annulus for each section in terms of laminar and turbulent flow, so frictional pressure losses will be calculated for each case and then the larger value will be considered as a result. The flow rates in the annulus across drillcollar and drillpipe, using Eq. 4.33 and considering respective effective annular velocity are given.

Laminar	*Turbulent*
Q_{dc}= 0.018502 m^3/sec	Q_{dc}= 0.019035 m^3/sec
Q_{dp}= 0.01087 m^3/sec	Q_{dp}= 0.01299 m^3/sec

Using Eq: 4.30 , the correction coefficient is calculated,

$(C_a)_{dc} = 0.97414$ $(C_a)_{dc} = 0.9746$

$(C_a)_{dp} = 0.9199$ $(C_a)_{dp} = 0.9277$

Newtonian viscosity is calculated using Eq: 4.32

μ_{dc}= 0.04255 (Pa.sec) μ_{dc} =0.04212 (Pa.sec)

μ_{dp}= 0.08615 (Pa.sec) μ_{dp} =0.08025 (Pa.sec)

$(Re)_{dc}$= 1849.85 $(Re)_{dc}$=1922.87 Using Eq: 4.31

$(Re)_{dp}$= 613.114 $(Re)_{dp}$=786.047

$(Re_{eq})_{dc}$= 1802.017 $(Re_{eq})_{dc}$= 1874.027 Using Eq: 4.29

$(Re_{eq})_{dp}$= 564.0608 $(Re_{eq})_{dp}$= 729.2772

Using Eq:4.35, Critical equivalent Reynolds numbers are calculated, which came out same for all cases, because it is only dependent to fluid parameter (n). The terms *y* and *z* are same as mentioned before.

Re_{eqcr} = 3582.62

After applying flow criteria, all sections showed laminar flow profile, So using Eq: 4.37 fanning friction factor (*f*) and then using Eq: 4.36 pressure losses are calculated.

$(f)_{dc}$= 0.01561 , $(\Delta p)_{dc}$= 4.89719 bar

$(f)_{dc}$= 0.01501 , $(\Delta p)_{dc}$= 4.9845 bar

$(f)_{dp}$= 0.04985 , $(\Delta p)_{dp}$= 16.064 bar

$(f)_{dp}$= 0.03856 , $(\Delta p)_{dp}$= 17.721 bar

The higher pressure losses are chosen from above results for each section, so across drill collar section the frictional pressure loss is calculated as $(\Delta p)_{dc}$= 4.9845 bar (73.0236 psi) and across the drill pipe, value is $(\Delta p)_{dp}$= 17.7213 bar (259.6172 psi).

Once the pressure losses for each section inside pipe and inside annulus are determined, the values are summed to give the total pressure losses. The results are summarized in Table5.3.

Table 5.3: Swab pressure when annular flow fraction (f_a) is 0.5.

fa	0.5	
	bar	**psi**
ΔPb	30.02	439.82
ΔPdc	5.15	75.54
ΔPdp	24.67	361.46
Total ΔPi	**59.85**	**876.82**
ΔPdca	4.98	73.02
ΔPdpa	17.72	259.61
Total ΔPa	**22.71**	**332.64**

Value of f_a is tried until total frictional pressure losses in the pipe interior and in the annulus become equal, for this purpose What-If analysis function in MS Excel is implied and calculations are performed again, considering the acceptable tolerance of 1psi or 0.068 bar difference. The final results are summarized in Table 5.4.

Table 5.4: Analytical results for swab pressure when f_a is 0.708.

fa	0.708	
	bar	**psi**
ΔPb	10.45	153.2
ΔPdc	2.19	32.19
ΔPdp	14.5	212.29
Total ΔPi	**27.14**	**397.58**
ΔPdca	5.76	84.46
ΔPdpa	21.31	312.11
Total ΔPa	**27.07**	**396.57**

Hence the results indicate that the total pressure loss beneath the drillstring due to upward movement of pipe is 397 psi and 70.8% of the flow at the bottom of drill string is from the annulus and 29.2% of flow is from the interior of the drill string.

5.2 Paradigm Sysdrill Solution

The same data for the example is also evaluated with the Paradigm Sysdrill software, the necessary steps are described below.

Create *New operator* → *Field* → *Installation* → *Slot* → *Well* → *Planned wellbore* → *Projects* → *New hydraulic calculations*, as shown in Figure 5.3.

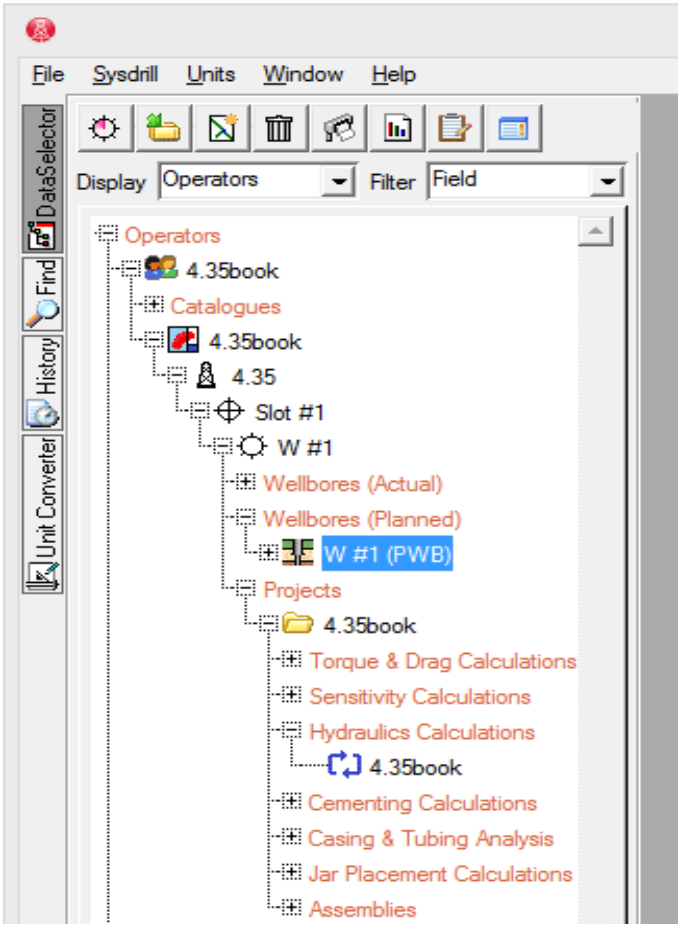

Figure 5.3 : Creating engineering project in Sysdrill.

In "*Planned wellbore*" dialogue, insert "*Hole section/casing*" particulars, shown in Figure 5.4. Drill string configuration is defined in "*Assembly dialogue*" , Figure 5.5.

After creating New Hydraulic calculation, select particular wellbore, wellpath, assembly and Rig data. Go to *Fluid Builder option* → *Rheology Tab* → *Test* → *Fann Data.*

Insert the viscometer dial readings, choose Herschel-Bulkley model and click on calculate symbol to find rheological parameters, as shown in Figure 5.1.

In Hydraulic calculation screen window, go to "*Circulating fluid*" insert density and select fluid model.

In "*Inputs*" tag insert the relevant data like depth, Bit TFA, RIH, POOH and click on the "*Calculate*" symbol, which results the surge and swab pressures in terms of equivalent density, as shown in Figure 5.7.

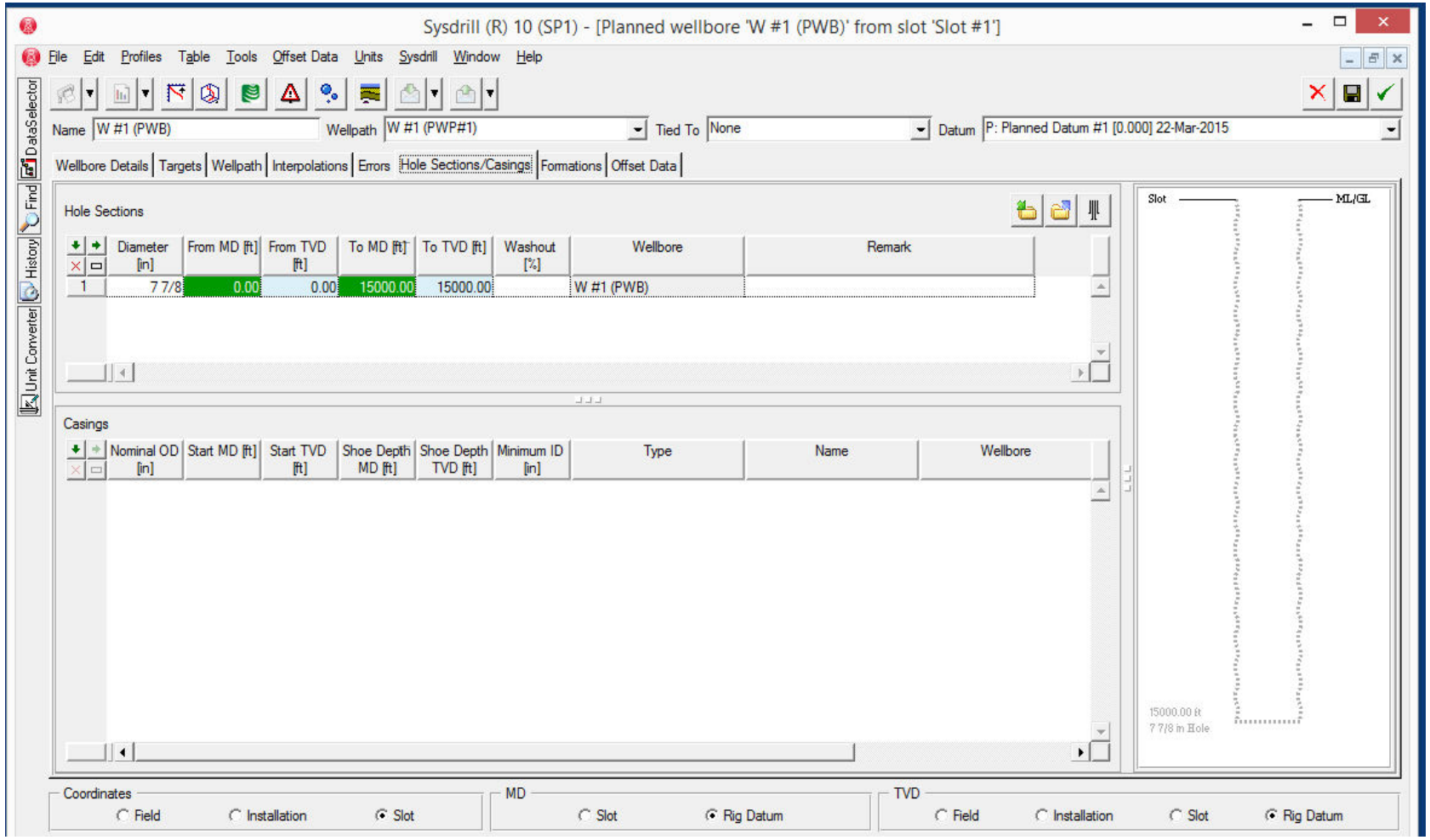

Figure 5.4 : Hole/casing section.

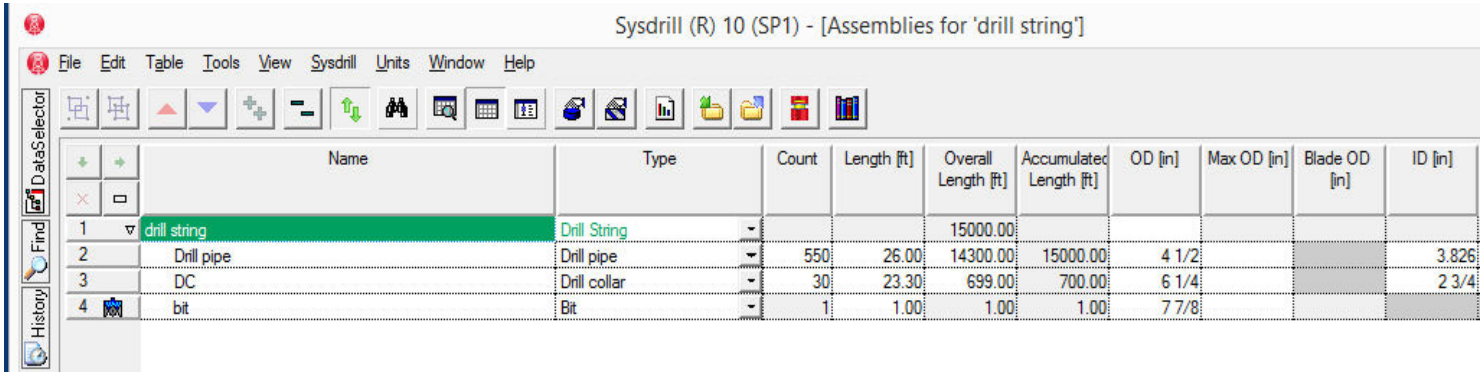

Figure 5.5 : Assembly/ Drill string tab.

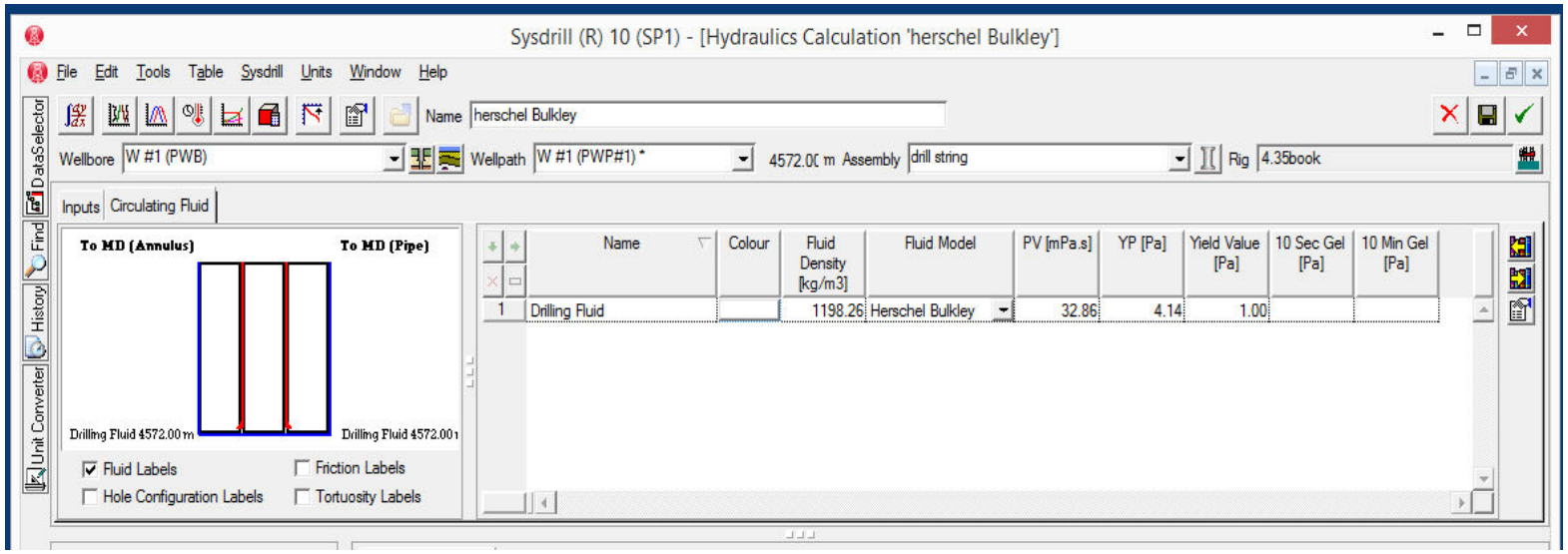

Figure 5.6 : Defining fluid model.

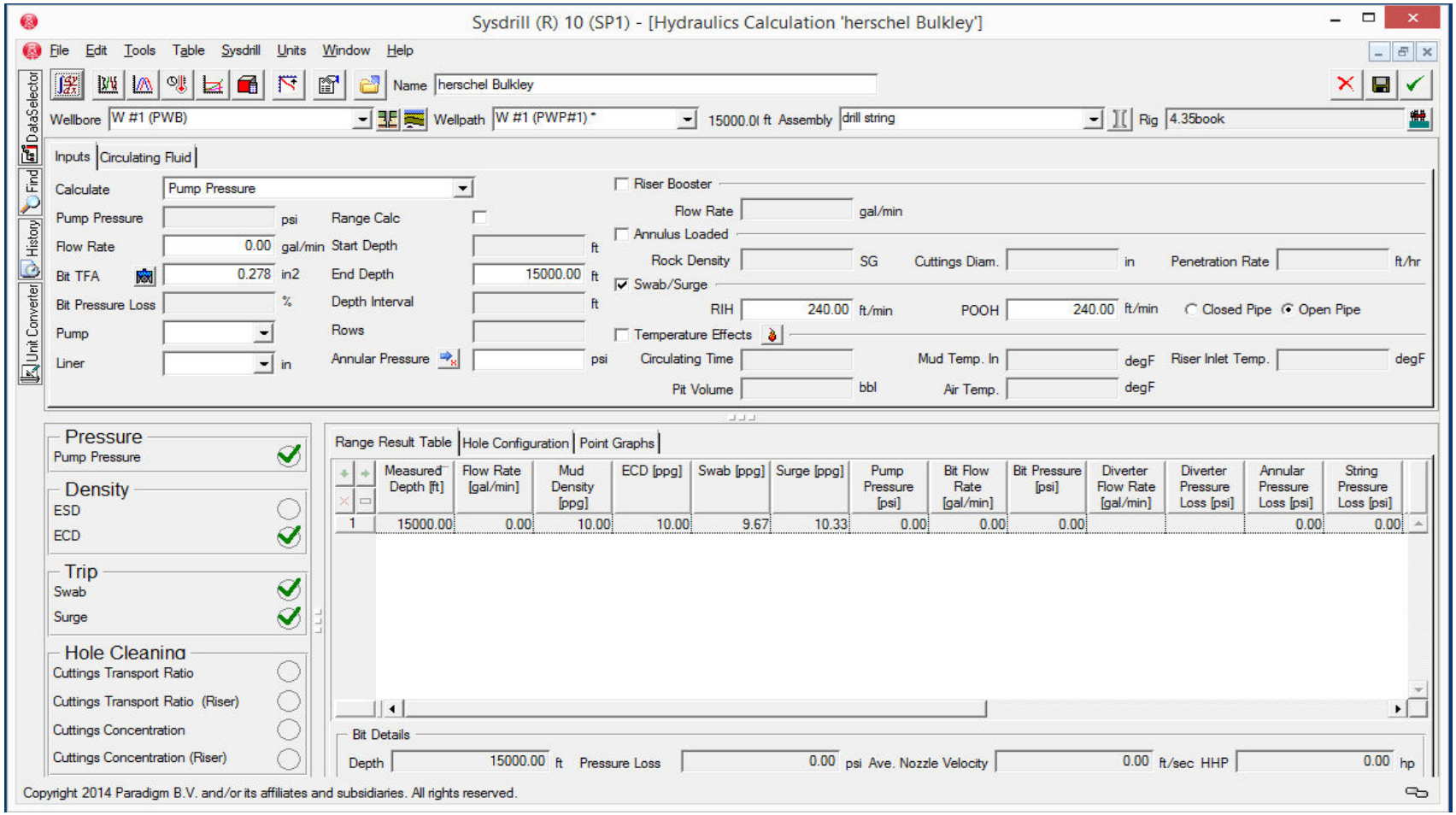

Figure 5.7 : Calculating pressure surges.

5.3 Sensitivity Analysis

The effect of tripping speed (V_p), bore hole clearance, effect of temperature and fluid density effects are investigated using Herschel Bulkley analytical model.

5.3.1 Comparision with other models

The swab pressure is also calculated for same wellbore configuration and drilling mud descibed in Table 5.2, for Bingham plastic and Power law models in order to make comparision.

The unweighted sepiolite mud, that is aged at the temperature of 150°F, has been used for the calculation, and abbreviated as UWSM150. The rheological parameters for Bingham Plastic and Power law are given in API units as,

Bingham Plastic Model: Plastic viscosity (μ_p) = 32.86cp,

Yield point (τ_y) = 8.66lb/100ft^2.

Power Law model: n= 0.54, K= 775.68 cp

The equations used for finding frictional pressure losses are taken from Bourgoyne (1991) text book.

Table 5.5: Analytical results with Bingham Plastic and Power Law models.

For Bingham Plastic		**For Power Law**	
fa	**0.714**	**fa**	**0.716**
ΔPb	148.04	ΔPb	146.13
ΔPdp	210.52	ΔPdp	234.56
ΔPdc	34.31	ΔPdc	30.87
Total ΔPi (psi)	**392.87**	**Total ΔPi (psi)**	**411.57**
ΔPdpa	285.85	ΔPdpa	324.7
ΔPdca	105.84	ΔPdca	87.96
Total ΔPa	**391.7**	**Total ΔPa**	**412.67**

After finding results from Paradigm sysdrill aswell, the summarized results are given in Table5.6,

Table 5.6: Swab pressure comparison with HB to other models for UWSM150.

	fa	Analytical (psi)	Sysdrill (psi)
Bingham Plastic	0.714	392.87	280.8
Power Law	0.716	412.67	218.4
Herschel Bulkley	0.708	397.58	257.4

The statistical results taken from Paradigm Sysdrill for UWSM150 are as under, as shown here the fit coefficient (R^2) is highest for Herschel Bulkley (i.e. 0.9997) among other models, so the swab pressure calculated with it's analytical solution would be appropriate. R^2 is a statistical method to find, how close the data is to regression line, which indicates the goodness of fit, and 0% means no match, while 100% means best fit.

Statistical Results

	Power Law	Bingham Plastic	Herschel Bulkley
Abs Ave Error %	5.4096	38.3396	1.3804
Sum Diff Sqd	8.0092	25.6176	0.2424
Fit Coeff (R2)	0.9903	0.9691	0.9997
St Dev Error	1.2448	2.2635	0.2202

Figure 5.8 : Statistical results for UWSM150.

5.3.2 Effect of tripping speed

One of most important parameter in pressure surges is tripping speed, the swab pressure for the open end pipe condition is calculated with Herschel-Bulkley model considering same wellbore and mud configuration, the density of fluid is taken constant as 10 ppg. The UWSM150 has been used for this calculation.

Table 5.7: Effect of pipe speed for open end condition.

Vp (ft/sec)	Sysdrill (psi)	Analytical (psi)	Annular flow fraction (fa)
1.5	156	210	0.59
4	257.4	397.6	0.709
6	319.8	547	0.751
10	507	1040.8	0.785
20	1115.4	3281	0.798

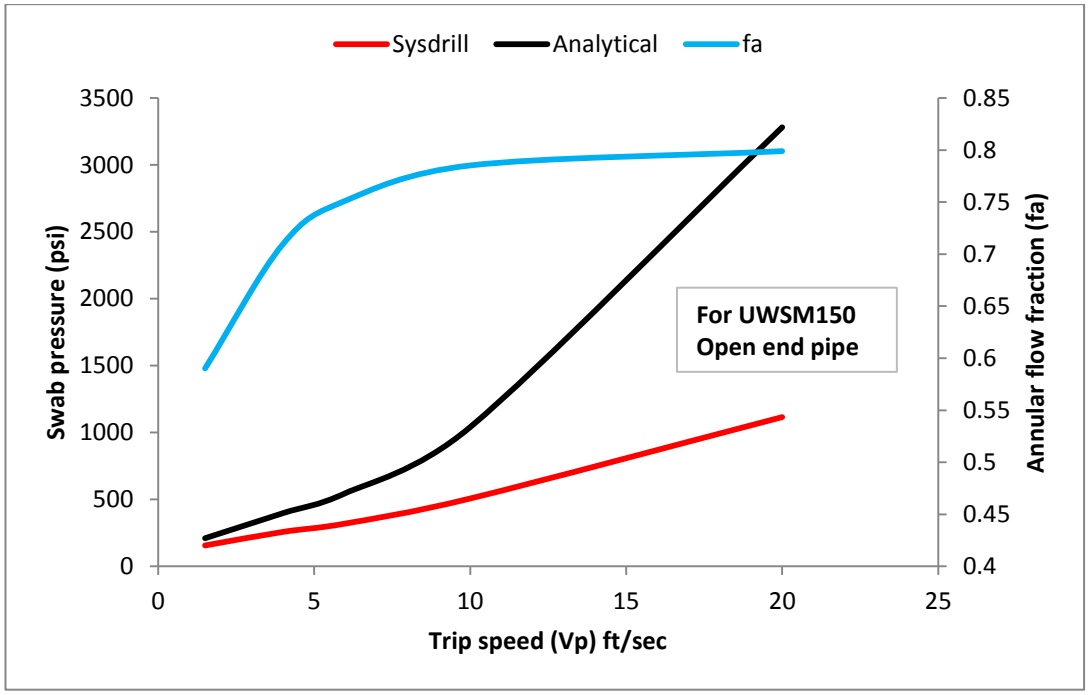

Figure 5.9 : Trip speed vs. swab pressure using HB model for UWSM150.

To understand the condition if bottom of the drill string is not open ended, which means through the pipe interior, no flow occurs and f_a is taken as one. Total flow is based on outer diameter of the pipe. Examples of such situation in the well with a check valve (float valve) present in the pipe string. For this condition the total flow rate is given by the following equation rather than Eq: 5.1, also no need to find mean and effective fluid velocities inside the drillcollar and drillpipe, then continue with the same steps from Eq:5.7 onward for finding mean and effective annular velocities, as describes before.

$$q_t = v_p \left[\frac{\pi}{4} (d_1)^2 \right] \qquad \textbf{(5.11)}$$

The effect on swab pressure for the closed end pipe condition is also studied for anayltical solution and results are tabulated. The wellbore specifications kept same as described above.

Table 5.8: Analytical results for swab pressures in open and close end condition.

Vp (ft/sec)	Open pipe	Close pipe
1.5	209.95	270.73
4	397.58	478.27
6	547.02	675.4
10	1040.77	1473.61
20	3281.69	4538.77

The graphical representation of taken results are as under.

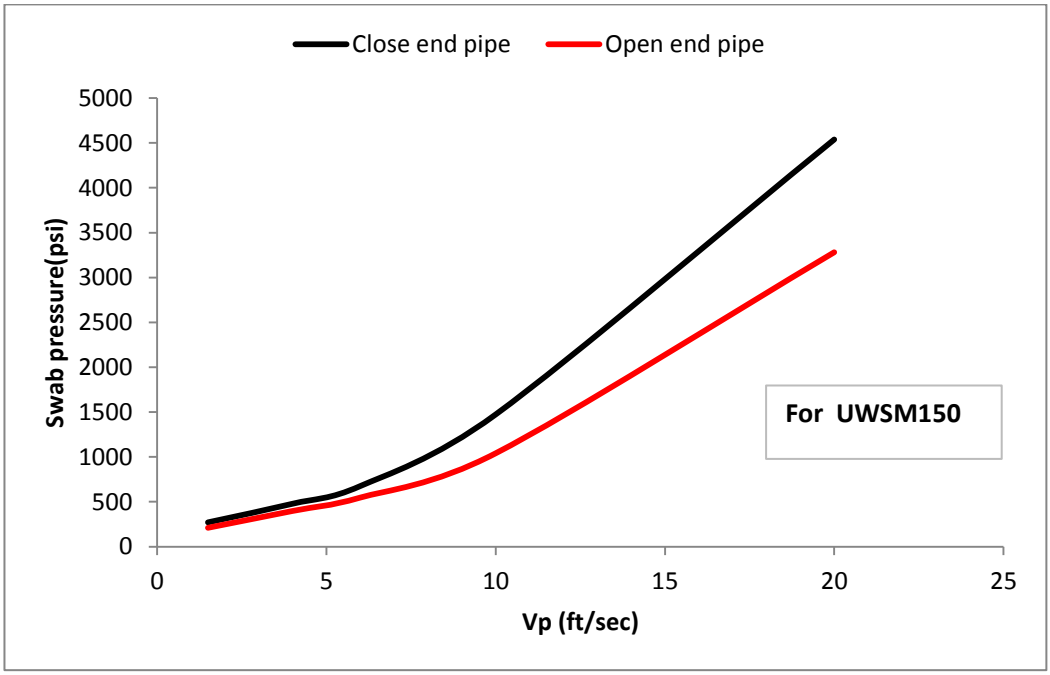

Figure 5.10 : Open end pipe vs. close end pipe using HB analytical model.

As shown from the results, by increasing tripping speed the swab pressure also increase. The removal of pipe from borehole at high speed causes higher swab pressure, which may result in well kick, if speed is not selected properly.

5.3.3 Effect of hole clearance

Hole clearance means the annuluar diameter is increasing around the drill string. Its effect is examined by keeping speed constant that is 4 ft/sec and same wellbore and drillstring configuration. The UWSM150 has been used for this calculation.

Table 5.9: Effect of hole clearance on swab pressure.

Diameter (inch)	Sysdrill (psi)	Analytical (psi)	Annular flow fraction (fa)
7.875	257.4	397.58	0.708
8.75	140.4	256.45	0.81
9.875	85.8	167.34	0.891
11	54.6	119.11	0.94
12.25	39	87.32	0.971

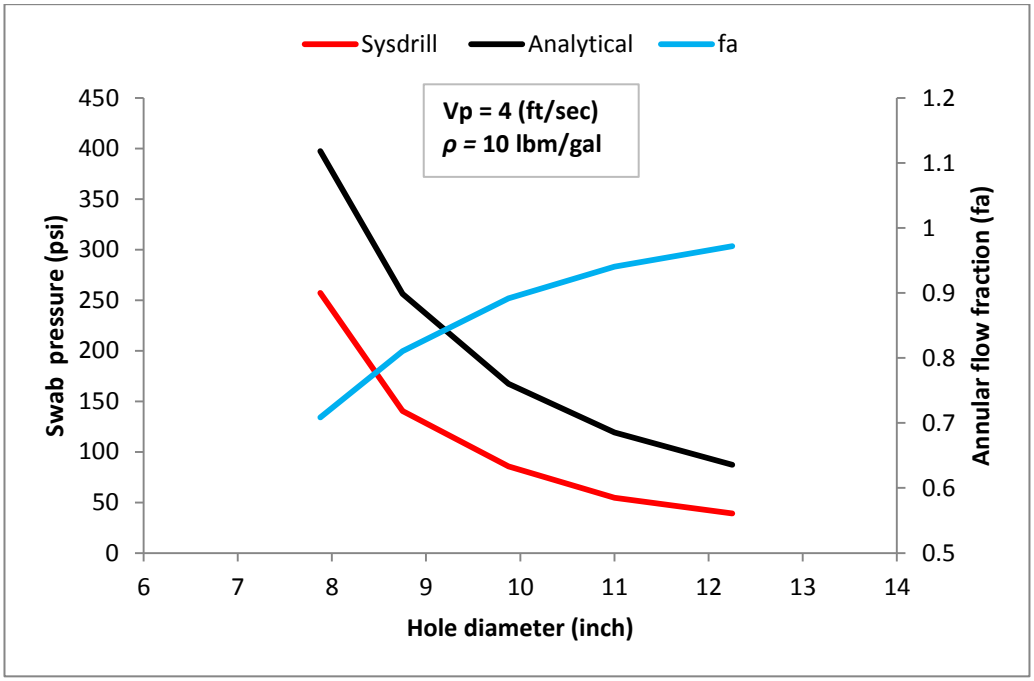

Figure 5.11 : Hole diameter vs. swab pressure for UWSM150.

The swab pressure is reducing with decreasing hole diameter, which means higher the hole clearence (space between drill string and formation/casing wall), lower will be the pressure surges.

5.3.4 Effect of fluid density

In the deeper wells, to maintain the formation pressure usually the density of drilling fluid is increased, which results in varying frictional pressure losses. To examine the effect of density on swab pressure is presented. The Herschel Bulkley analytical model is used to calculate using trip speed of 4 ft/sec, other wellbore and drill string particulars kept same. The rheological properties of UWSM150 has been used for this calculation.

Table 5.10 : Effect of fluid density on swab pressure.

Density (ppg)	Pressures with HB model (psi)	
	UWSM150	WSM150
8.6	392.7	528
10	397.58	534
12	402.3	541.2
14	409.13	547
16	421.23	552
18	432.2	556.3

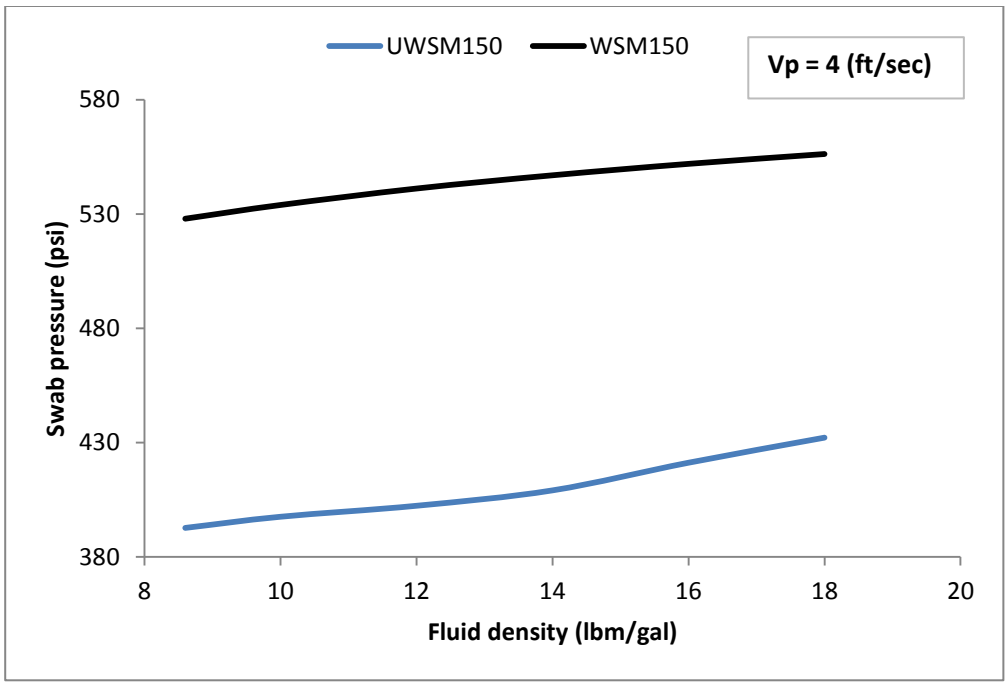

Figure 5.12 : Effect of fluid density on swab pressure.

As shown in figure the pressure surges are proportional to the fluid density. With increasing density of the fluid, the swab pressure is also enhancing, so this is an other important parameter which should be considered while increasing mud weight during drilling.

5.3.5 Effect of temperature

The rheological properties of a sepiolite drilling mud is examined at different temperatures in order to investigate the effect of temperature variations on swab pressure. The purpose is to demonstrate the situation, as if drilling mud is being exposed to high temperature formations during drilling. The tests are conducted both with viscometer and rheometer.

<u>Test Performed Using Fann35A Viscometer</u>

An unweighted sepiolite mud is formed with the composition mentioned in Table A.1. Then sample is placed in a aging cell and kept inside heating oven at respective temperatures for 16 hours then cooled back to atmospheric conditions, just after that rheology is examined using Couette type viscometer, which is the product of Fann instruments with the brand name of Fann35 rotational viscometer. The picture of the instrument is shown in Figure 5.13.

Figure 5.13 : Fann35A rotational viscometer.

Herschel-Bulkley model parameters are calculated from observed dial readings using Sysdrill *Fluid Builder* option as discussed before. The results for UWSM is given in Table 5.11.

Table 5.11 : UWSM viscometer readings and HB model parameters.

	100 °F	150°F	200°F	250°F	300°F	350°F	400°F	450°F
RPM				**Dial Readings**				
600	71	70	59	46	38	39	47	52
300	45	44	38	30	24	26	31	35
200	35	35	30	23	18	20	25	29
100	22	23	20	15	11	13	17	21
6	5	5	4	4	3	3	5	7
3	4	4	3	3	2	2	4	6
n	0.68	0.66	0.63	0.67	0.72	0.62	0.62	0.59
K (mPa.s)	310.39	349.68	379.85	223	124.42	263.31	297.87	404.82
τ_y (Pa)	1.05	1	0.46	0.91	0.7	0.33	1.26	2.03
R^2	0.9999	0.9997	0.9999	0.9999	0.9995	0.9998	0.9999	0.9995

The swab pressures are calculated using fluid model parameters given in Table 5.11, with both analytical and Sysdrill software. The speed is taken as 4 ft/sec and density of fluid is 10 lbm/gal, other wellbore specification kept same.

Table 5.12 : Swab pressure using Sysdrill and HB model for UWSM with viscometer readings.

	100 °F	150°F	200°F	250°F	300°F	350°F	400°F	450°F
Sysdrill	249.6	257.4	218.4	179.4	132.6	148.2	210.6	265.2
HB	392.02	397.6	353.5	287.92	226.85	248.94	308.84	381.12

The graphical representation of result is given in Figure 5.14.

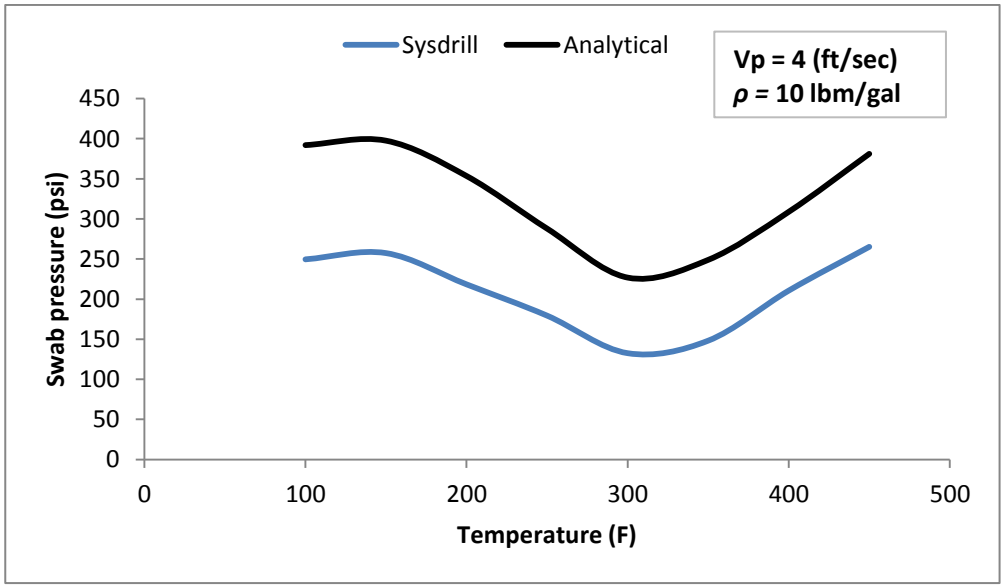

Figure 5.14 : Analytical vs. Sysdrill for UWSM using Fann35A results.

The examination is further extended to evaluate the effect of weighted sepiolite drilling mud. Similar method is performed and the composition of mud is taken as given in Table A.2.

Table 5.13 : WSM viscometer readings and HB model parameters.

	100 °F	150°F	200°F	250°F	300°F	350°F	400°F	450°F
RPM				**Dial Readings**				
600	104	91	72	59	52	50	64	70
300	68	59	45	36	31	29	44	50
200	53	46	34	27	23	21	35	38
100	35	30	21	17	14	12	23	26
6	9	7	4	3	3	3	7	9
3	6	5	3	2	3	3	6	8
n	0.64	0.65	0.7	0.72	0.79	0.86	0.61	0.61
K(mPa.s)	610.65	515.3	276.1	200.03	106.75	64.04	465.71	486.96
τ_y (Pa)	1.59	1.16	0.62	0.43	1	1.13	1.69	2.6
R^2	0.9999	1	0.9999	1	0.9999	0.9997	0.9994	0.998

Again for this type of mud, swab pressure is calculated with both Herschel-Bulkley analytical model and Sysdrill software.

Table 5.14 : Swab pressures using Sysdrill and HB model for WSM with viscometer readings.

	100 °F	150°F	200°F	250°F	300°F	350°F	400°F	450°F
Sysdrill	397.8	335.4	226.2	171.6	156	140.4	296.4	343.2
HB	612.2	534.2	367.7	296.08	269.27	253.74	441.6	492.92

The graph is constructed as shown in Figure 5.15. The swab pressure seems to have same trend both for Sysdrill and HB model, but Sysdrill is giving lower values as compare to other one. As temperature is increasing till 350°F, swab pressure is decreasing which is the result of reducing fluid viscosity and in result reducing frictional pressure losses, but after this point again pressure is showing an inclination in trend. The reason may be the gelling effect or flocculation of chemicals other than sepiolite present in the mud, because study (Altun et al.) has shown the stability of sepiolite till 500°F if used alone.

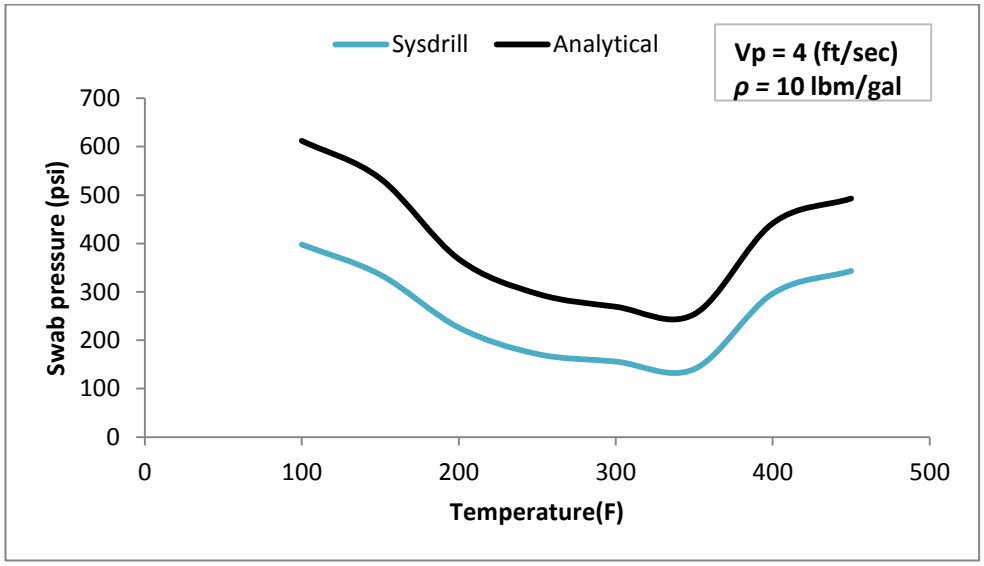

Figure 5.15 : Analytical vs. Sysdrill for WSM using Fann35A results.

In order to compare results for both type of mud simultenously, the results taken from analtical method are plotted against each other and shown in Figure 5.16.

Table 5.15 : Swab pressure for UWSM and WSM with viscometer readings using analytical model.

	100 °F	150°F	200°F	250°F	300°F	350°F	400°F	450°F
Unweighted	392.02	397.6	353.5	287.92	226.85	248.94	308.84	381.12
Weighted	612.2	534.2	367.7	296.08	269.27	253.74	441.6	492.92

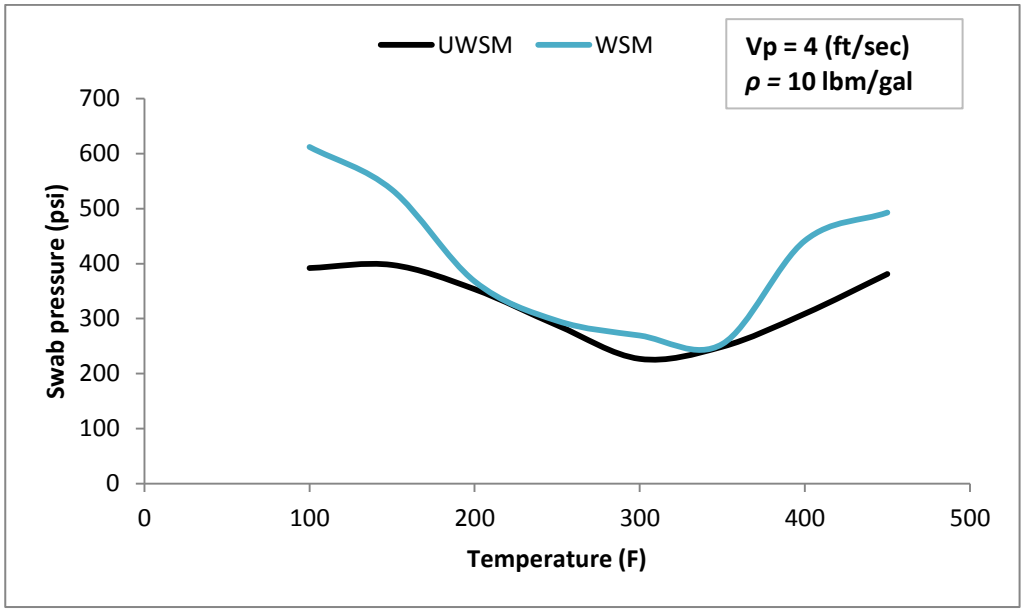

Figure 5.16 : UWSM vs. WSM using analytical model for viscometer results.

Test Performed Using Fann50SL Rheometer

The rheological properties of unweighted sepiolite mud is calculated using high temperature and high pressure (HTHP) rheometer. A mud sample is formed with the composition mentioned in Table A.1. A rheometer simulate the real formation temperature conditions and compute mud rheology at dynamic conditions. A sample is placed inside the sample chamber in rheometer without aging it, and after connecting with the integerated computer program and feeding necessary parameters. The picture of the instrument is shown in Figure 5.17. The shear stresses are computed automatically with the gradual increase of temperatue (i.e:10°F). Here for the convenience, readings for the temperatures with the interval of 50°F are taken. Herschel-Bulkley model parameters are calculated from observed shear stresses using Sysdrill "*Fluid Builder*" option, the shear stress and shear rate values are inserted instead of RPM and dial readings. The results are given in Table 5.16.

Figure 5.17 : Fann50SL HTHP rheometer.

Table 5.16: UWSM rheology and H.B model parameters using rheometer.

	100 °F	150°F	200°F	250°F	300°F	350°F	400°F	450°F
Shear Rates (1/sec)				**Shear Stress (Pa)**				
1021.65	68.90	48.24	34.16	21.61	12.57	8.08	15.73	21.06
510.82	41.02	28.08	19.59	11.56	6.23	3.83	10.33	14.67
340.55	30.78	21.27	15.02	8.42	4.14	2.44	9.19	12.51
170.27	19.36	13.49	9.70	4.96	2.11	1.08	7.82	10.45
10.22	3.79	2.37	1.57	0.28	-0.35	-0.43	7.55	13.03
5.11	3.13	1.73	1.11	-0.02	-0.51	-0.53	9.50	15.13
n	0.76	0.77	0.77	1	1.03	1.13	1.97	2.79
K (mPa.s)	337.62	230.5	164.5	19.39	9.57	3.33	0.01	0.01
τy (Pa)	1.94	1.04	0.67	1.68	0.16	0.1	8.27	12.81
R^2	0.9999	0.9995	0.9989	0.9999	1	0.9991	0.9438	0.8154

The swab pressure is calculated using these fluid model parameters with both analytical and Sysdrill software. The speed is taken as 4 ft/sec and density of fluid is 10 lbm/gal, other wellbore specification kept same. The results are shown below,

Table 5.17 : Swab pressures using Sysdrill and HB model for UWSM with rheometer readings.

	100 °F	150°F	200°F	250°F	300°F	350°F	400°F	450°F
Sysdrill	390	257.4	187.2	132.6	62.4	62.4	312	460.2
HB	617.08	439.57	319.2	247.5	202.57	186	406.2	534

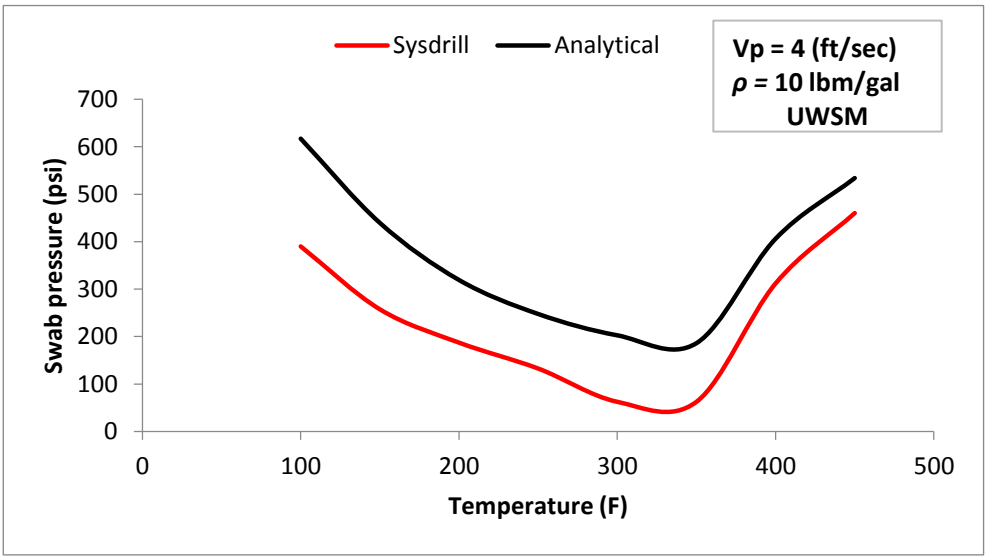

Figure 5.18 : Analytical vs. Sysdrill for UWSM using Fann50SL results.

Now weighted sepiolite mud is evaluated using similar test procedure.

Table 5.18: WSM rheology and H.B model parameters using rheometer.

	100 °F	150°F	200°F	250°F	300°F	350°F	400°F	450°F
Shear Rates (1/sec)				**Shear Stress (Pa)**				
1021.65	101.35	63.83	42.64	26.24	15.02	9.60	24.09	25.58
510.82	63.45	39.48	25.31	14.09	7.38	4.40	17.32	17.73
340.55	49.74	30.30	18.87	9.99	4.88	2.63	16.11	15.44
170.27	32.70	19.72	12.15	5.79	2.60	1.09	15.32	13.40
10.22	7.44	4.13	2.13	0.70	0.16	-0.46	19.44	16.02
5.11	6.00	3.15	1.52	0.33	-0.02	-0.63	19.08	17.24
n	0.68	0.7	0.75	0.89	1.08	1.22	1.99	1.22
K (mPa.s)	863.23	476.89	226.18	56.35	7.91	2.08	0.01	2.86
τy (Pa)	3.39	1.72	0.86	0.21	0.51	0.1	15.07	11.86
R^2	0.9998	0.9999	0.9997	0.9997	1	0.9976	0.9999	0.9995

Again for this type of mud, swab pressure is calculated with both Herschel-Bulkley analytical model and Sysdrill software.

In Table 5.16 and 5.18, it can be noticed that at some temperatures, negative values for shear stresses are observed, which is only present in rheometer results. This is due to the "*wall slip effect*" in the Couette type rheometer. The water based mud usually demonstrate a significant amount of wall slip because of phase separation at higher temperatures.

Table 5.19 : Swab pressures using Sysdrill and HB model for WSM with rheometer readings.

	100 °F	150°F	200°F	250°F	300°F	350°F	400°F	450°F
Sysdrill	694.2	405.6	234	101.4	78	62.4	514.8	421.2
HB	1022.76	636.2	392.16	232	215.34	197	589.6	505.5

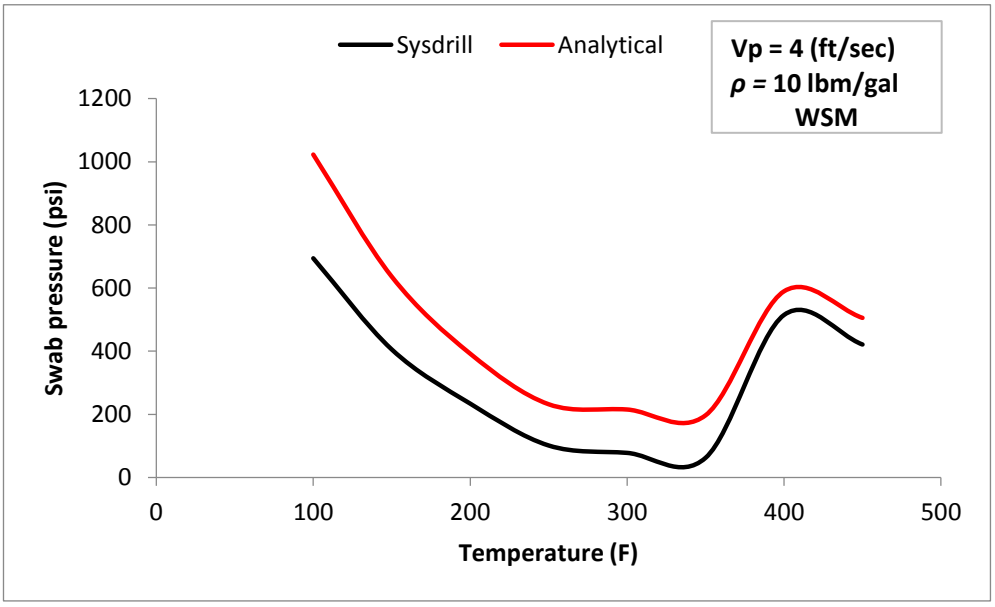

Figure 5.19 : Analytical vs. Sysdrill for WSM using Fann50SL results.

To compare the results of unweighted and weighted mud, the analytical results are tabulated and given in Table 5.20.

Table 5.20: Swab pressures for UWSM and WSM with rheometer readings.

	100 °F	150°F	200°F	250°F	300°F	350°F	400°F	450°F
Unweighted	617.08	439.57	319.2	247.5	202.57	186	406.2	534
Weighted	1022.76	636.2	392.16	232	215.34	197	589.6	505.5

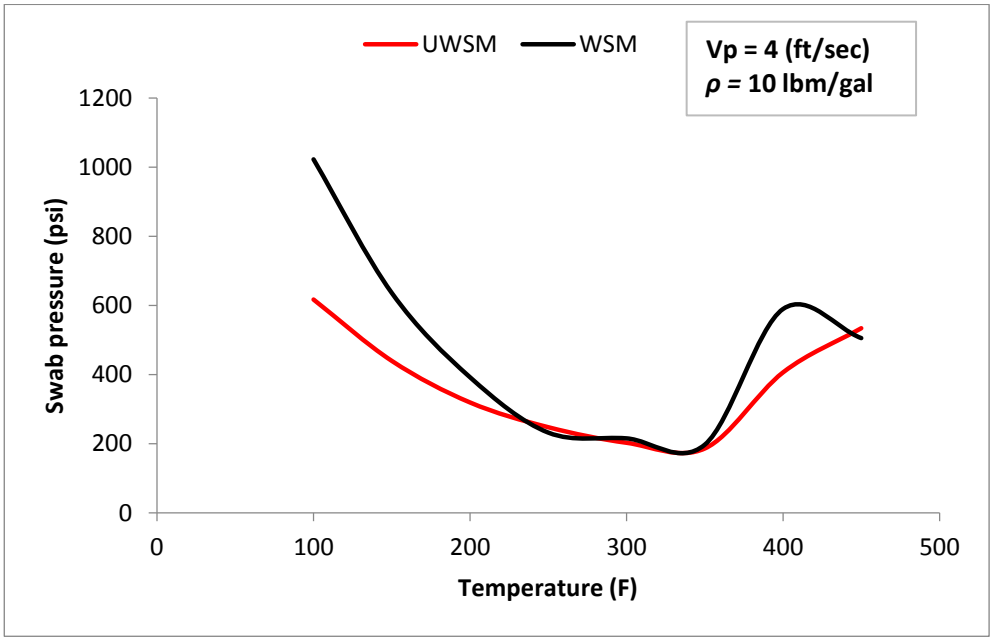

Figure 5.20 : UWSM vs. WSM using analytical model for rheometer results.

Comparision of Viscometer and Rheometer Results

The results taken from rotational viscometer and rheometer are compared both for unweighted and weighted mud. For unweighted sepiolite mud the results are plotted and given in Figure 5.21.

Table 5.21 : Swab pressure calculated using viscometer and rheometer results for UWSM.

	100 °F	150°F	200°F	250°F	300°F	350°F	400°F	450°F
Fann35	392.02	397.6	353.5	287.92	226.85	248.94	308.84	381.12
Rheometer	617.08	439.57	319.2	247.5	202.57	186	406.2	534

Now the swab pressure results calculated using weighted mud are given in Table 5.22

Table 5.22 : Swab pressure calculated using viscometer and rheometer results for WSM.

	100 °F	150°F	200°F	250°F	300°F	350°F	400°F	450°F
Fann35	612.2	534.2	367.7	296.08	269.27	253.74	441.6	492.92
Rheometer	1022.76	636.2	392.16	232	215.34	197	589.6	505.5

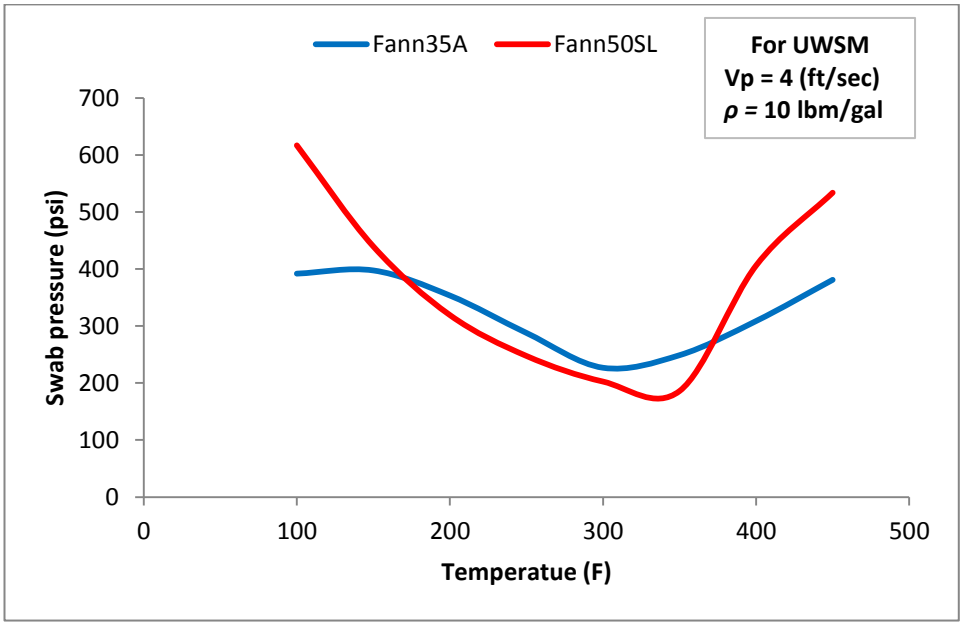

Figure 5.21 : Viscometer vs. Rheometer results for UWSM using analytical model.

The rheometers is exhibiting higher swab pressures at the beginning compare to rotational viscometer, but in between the temperature values of 150°F to 350°F, exhibiting lower values.

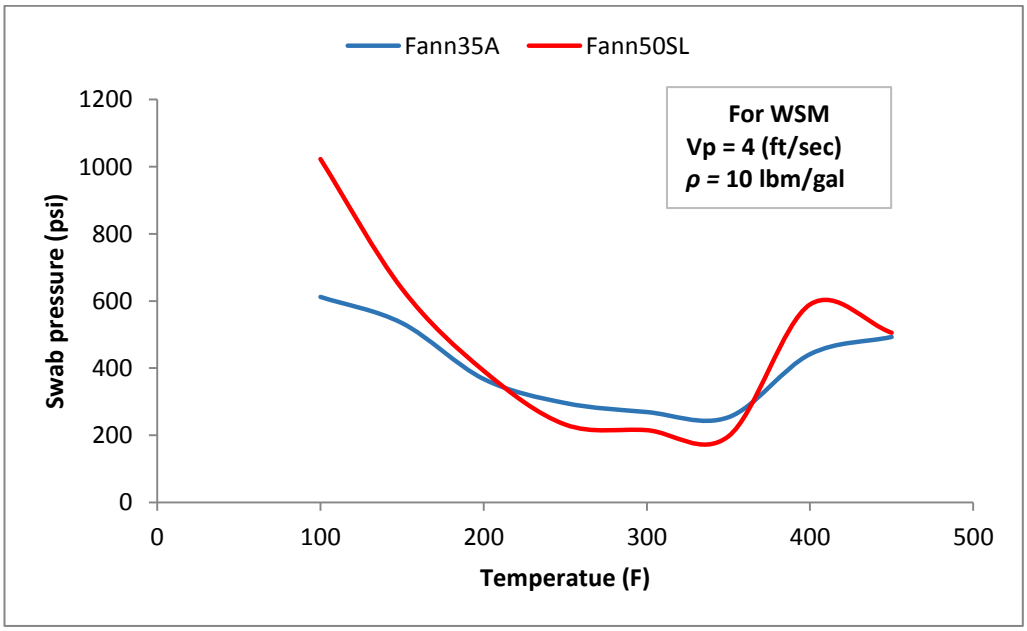

Figure 5.22 : Viscometer vs. Rheometer results for WSM using analytical model.

For weighted sepiolite mud, the comparison of results taken from viscometer and rheometer is showing a unique trend, swab pressure tend to decrease till 350°F for rheometer data, and again decline is observed in between 400°F to 450°F, after a

sharp increase. The rheometer displays more realistic conditions of formation temperature as compare to the viscometer so, it is better to rely on the mud rheology measured with rheometer. For WSM, both temperature and density is affecting on swab pressures that's why the values are higher as compare to UWSM.

6. RESULTS AND DISCUSSIONS

The results from the Herschel-Bulkley analytical model is found to be varying from the values obtained from Paradigm Sysdrill software. Not only for Herschel Bulkley, but even for Bingham Plastic and Power Law rheological models, software results in lower pressure values, compare to pressures calculated using analytical methods.

In fact the formulations which software is using, are not been exposed due to its commercial integrity but according to the paradigm technical support department, the software is lagging in calculating accurate surge and swab pressures, which they admitted in response of email correspondence. The part of email reply, responded by one of their technical person is, "*We are making patch to the software that will be available later in the year and we will update the code accordingly. Other fixes will include fixing a gross error in the temperature model and inclusion of the eccentric flow corrections for annular pressure loss for slim hole conditions.*" They informed to overcome this problem in next upcoming version, so the results taken from Herschel Bulkley analytical model came out to be reliable.

Generally speaking, the steady flow model is conservative in nature and normally does not consider the factors such as; 1) fluid compressibility, 2) fluid inertia, 3) pipe longitudinal elasticity. Dynamic surge models, while giving less conservative predictions, are more complex and require not only more input data, which may not be readily available to engineers, but also more computer resources (Mitchell, 1988).

As shown in Figure 5.9, the effect of tripping speed is vital. The values greater than 10 ft/sec are taken just for getting idea, otherwise they are unrealistic speeds. The swab pressure is increasing with increasing tripping speed. It can also be seen that the annular fraction flow is rising, which means that the drilling fluid starts displacing more from the annulus rather than from pipe interior. The tripping with close ended pipe has more effect on surge pressures, as compare to open ended pipe, shown in Figure 5.10.

Hole diameter has shown pronounced effect on swab pressure as shown in Fig. 5.11.

The increase in annular clearance decreases the swab pressure significantly, and increases the annular flow fraction.

The effect of fluid density on swab pressures has shown a minimal change. By increasing the density of drilling fluid for both UWSM150 and WSM150, the swab pressures are also increasing, and WSM150 has more pressure values compare to UWSM150, at the same tripping speed.

Every one involves in drilling operations knows that, muds behave with non-Newtonian fluid flow properties. Their viscosity is not only influenced by temperature and pressure, but it is also strongly related to the velocity at which mud runs inside the hydraulic system. The drilling fluid velocity and the resulting rate of shear at the walls of the conducts, plays an important role on the viscosity of the fluid. For this reason, the full range of shear rate usually considered for hydraulic calculations. At least three data points of shear rates are required to calculate Herschel Bulkey rheological constants, here six different values for shear rates have been utilized for the examination

The temperature effect on swab pressure also seems unique, as Figures 5.14, shows that for UWSM using viscometer dial readings, swab pressure is lowering till 300°F and then increasing again. Similarly, Figures 5.15, 5.18 and 5.19 show a trend that for sepiolite mud, between 100°F to 350°F, the swab pressure is reducing and then increasing again. This reduction of swab pressure is due to the decrease of consistency index (K), which describes the thickness of fluid (as “K” decreases mud becomes thinner), which reflects that apparent viscosity is reducing and in turn swab pressure is also reducing.

The increase of swab pressure is due to the gelation effect of mud, which can be supported by the fact that yield stresses are also increasing after 350°F, as given in Tables 5.11, 5.13, 516 and 5.18.

It is observed that the apparent viscosity values of mud first decrease until 350°F, and then began to increase. The same situation is also experienced in the case of yield point and gel strength values. This behavior is one of the main characteristic properties of sepiolite clays. It is well known, that sepiolite begins to convert to a smectite at 300°F, and this reaction is fully completed at 500°F. The new smectite (thermally altered sepiolite clay) in the fluid have a thin flakey morphology, and they increase the viscosity of the fluid (Altun et al., 2014).

Figures 5.16 and 5.20, show the comparison results for UWSM and WSM, it can be observed that the effect of barite (weighing material) is getting diminish at some temperatures, which means that WSM and UWSM are resulting in almost same swab pressures at certain temperatures.

After a sharp increase again a drop down of swab pressure is observed for only WSM given in Figure 5.19, because of the reason that yield stress reduced as gelation effect disappeared at 400°F early as compare to UWSM, also the flow behavior index (*n*, that measures the degree to which the fluid is shear-thinning or shear-thickening) lowered, which can be seen in Table 5.18.

In Figures 5.21 and 22, while comparing the results for rotational viscometer (Fann35A) and HTHP rheometer (Fann50SL), it can be noticed that Fann50SL is giving lower swab pressures from 200°F to 350°F, as compare to Fann35A. In Table A.3 and A.4, the calculated values for flow behavior index, consistency index and yield stress are given both for unweighted sepiolite mud and weighted sepiolite mud. In Figure 5.21, the distance between two curves at the beginning and at the end, is due to the viscosity effect between UWSM and WSM.

It can be derived that the rheological parameters such as yield stress, fluid behavior index and consistency index have substantial effects on surge and swab pressures.

To predict how much trip speed can be increased if the formation temperature changes. For this purpose, the readings from rheometer are taken for comparison of UWSM and WSM at 350°F, and swab pressures are estimated using Herschel Bulkley analytical model. From Table 6.1, it is clear that swab pressure is decreasing from initial temperature around three times for UWSM and five times for WSM respectively, which allows to make an increase in trip speed.

Table 6.1 : Possible increase in trip speed for UWSM and WSM until 350°F.

UWSM350			**WSM350**		
Speed (ft/sec)	Temp.(F)	Swab press. (psi)	Speed (ft/sec)	Temp.(F)	Swab press.(psi)
4	100	617.08	4	100	1022.76
4	350	186	4	350	197
8	350	612.5	10	350	1018.34

As shown in Figure 6.1, the possible increase can be up to 8ft/sec for UWSM and 10 ft/sec for the WSM, and yielding almost the same amount of swab pressures.

It is determined that at the formation temperature up to 350°F, the use of both weighted and unweighted sepiolite muds allow to fasten the tripping speed of the drillstring.

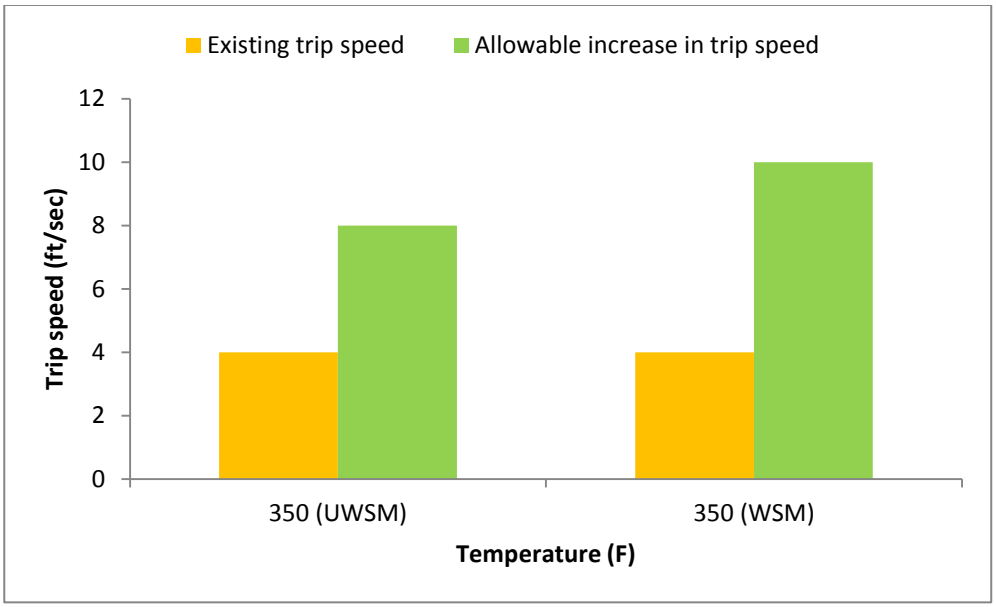

Figure 6.1 : Possible increase in trip speed at 350 °F.

As it is well known that "time is money", and in drilling industry this fact is well suited. In geothermal wells and deep offshore wells, the increase in tripping speed can save time, and in return significant amount of money.

7. CONCLUSION AND RECOMMENDATIONS

The conclusive remarks, derived from this study are as follows:

- Herschel-Bulkley analytical model results in better swab pressure prediction with compare to Paradigm Sysdrill, despite of the fact that it gave higher values, the results are reasonable and make it a conservative solution.
- Effect of tripping speed of pipe, and fluid density has direct relationship to swab pressure.
- If the space between borehole wall and drillstring (annular clearance) is larger, the swab pressure is exhibiting lower values.
- Swab pressure decreases, as formation temperature increases up to certain value.
- It is also determined that at the formation temperature up to 350°F, the use of both weighted and unweighted sepiolite muds allow to fasten the tripping speed of the drillstring.
- Mud rheological constants varying with elevated temperatures have substantial effect on surge/swab pressure calculations.
- Mud clinging constant graph is not available for Herschel-Bulkley model so far, which can be developed to predict more accurate frictional pressure losses.
- Investigation for different types of mud samples (i.e. KCL, Polymer based mud, Lignosulphonate mud), can be performed to compare results against sepiolite mud at higher temperatures.

REFERENCES

Bourgoyne, A.T., Chenevert, E.M., Millheim, K.K., and Young, F.S., (1991). "Applied Drilling Engineering*",* (SPE), Richardson, Texas.

Burkhardt, J.A., (1961). *"Wellbore pressure surges produced by pipe movement"*, Journal of Petroleum Technology,13(6), SPE-1546-G-PA, June 1961.

Canon, G.E., (1934) *"Changes in Hydrostatic pressure due to withdrawing drillpipe from hole"* API Drill and Prod. Practice.

Crespo, F. ; Ramadan A., *"Surge and swab pressure predictions for yield power law drilling fluid",* SPE Latin America and Caribbean petroleum conference (Dec. 2010).

Goins, W.C ; J.P. Weichhert; J.L.Burba *"Downhole pressure surges and their effect on loss of circulation"*, API Drill and Prod.Practice (1951).

Gursat Altun, Ali Ettehadi Osgouei, Mustafa Hakan Ozyurtkan, (2014). "*Customization of sepiolite based drilling fluids at high temperatures",* ARMA 14-7031, Geomechanics Symposium, Minneapolis, MN, USA, June 2014.

Gursat Altun, Ali Ettehadi Osgouei., (2014) *"Investigation and remediation of active-clay contaminated sepiolite drilling muds",*Journal of Applied Clay Science, CLAY3193, DOI: 10.1016/j.clay.2014.10.002.

Horn A.J. *"Well blowouts in california drilling operations,causes and suggestions for prevention"*, API Drill and Prod. Practice (1950).

Hussain Rabia, (2001). "Well Engineering and Construction*",* Entrac consulting.

Merlo.A, Maglione.R and Piatti.C, (1995). "*An innovative model for drilling fluid hydraulics".* Paper presented at the SPE Asia Pascific Oil & Gas conference,Kuala Lumpur, Malaysia, 20-22 March 1995.

Mitchell R.F. "*Dynamic surge and swab pressure predictions",* SPE Drilling Engineering (Sept. 1988).

Robert F. Mitchell, (2007). "Petroleum Engineering Handbook, Volume II, Drilling Engineering", SPE.

Skalle, P., (2012). "Drilling Fluid Engineering", Ventus publishing Aps.

Url-1 <*http://www.petrowiki.org*>*,* date retrieved 10.04.2015

Url-2 <*http://www.pdgm.com/products/sysdrill/*>, date retrieved 13.04.2015

APPENDICES

APPENDIX A.1 : Mud Clinging constant (K), for computing surge/swab pressure.

APPENDIX A.1

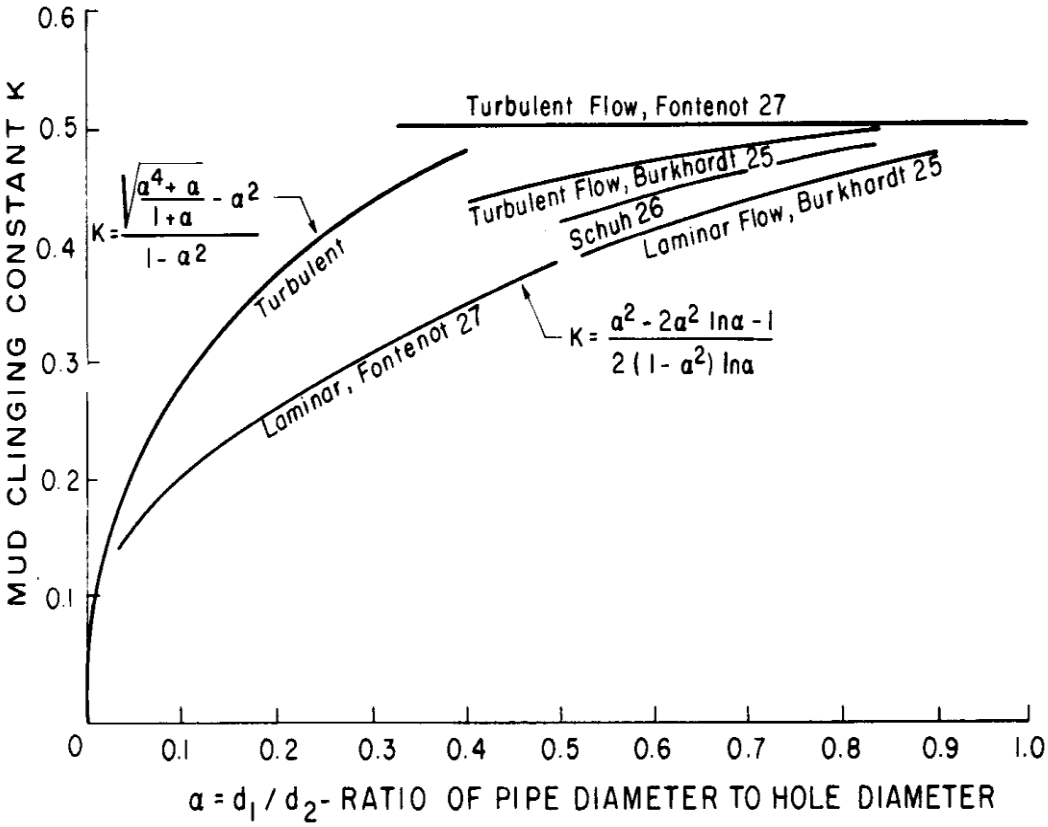

Figure A.1 : Mud clinging constant (K), for finding effective fluid velocity.

Table A.1 : Unweighted sepiolite mud composition (Altun, et al. 2014).

Composition	Quantity	Mixing Time (min)
Water	350 ml	
Sepiolite	20 gm	20
Soda Ash	0.1 gm	5
Thermatine	3.25 ml	5
Hostadrill	5 gm	5

Table A.2 : Weighted sepiolite mud composition (Altun, et al. 2014).

Composition	Quantity	Mixing Time (min)
Water	350 ml	
Sepiolite	20 gm	20
Barite	150 gm	10
Soda Ash	0.1 gm	5
Thermatine	3.25 ml	5
Hostadrill	5 gm	5

Table A.3 : Rheological constants for UWSM in field units.

Temperatures (°F)	Viscometer results			Rheometer results		
	n	K (cP)	τy (lbf/100ft2)	n	K (cP)	τy (lbf/100ft2)
100	0.68	310.39	2.2	0.76	337.62	4.05
150	0.66	349.68	2.1	0.77	230.5	2.17
200	0.63	379.85	0.97	0.77	164.5	1.4
250	0.67	223	1.9	1	19.39	3.5
300	0.72	124.42	1.5	1.03	9.57	0.33
350	0.62	263.31	0.7	1.13	3.33	0.21
400	0.62	297.87	2.6	1.97	0.01	17.27
450	0.59	404.82	4.2	2.79	0.01	26.75

Table A.4 : Rheological constants for WSM in field units.

Temperatures (°F)	Viscometer results			Rheometer results		
	n	K (cP)	τy (lbf/100ft2)	n	K (cP)	τy (lbf/100ft2)
100	0.64	610.65	3.32	0.68	863.23	7.08
150	0.65	515.3	2.42	0.7	476.89	3.6
200	0.7	276.1	1.3	0.75	226.18	1.8
250	0.72	200.03	0.89	0.89	56.35	0.43
300	0.79	106.75	2.08	1.08	7.91	1.06
350	0.86	64.04	2.36	1.22	2.08	0.2
400	0.61	465.71	3.5	1.99	0.01	31.4
450	0.61	486.96	5.4	1.22	2.86	24.7

CURRICULUM VITAE

Candidate's full name:	Muhammad Mubeen ur Rehman ARAIN
Place and date of birth:	Pakistan, 05 Feb 1987
Permanent Address:	Karachi, Sindh, Pakistan
Universities and Colleges attended:	• M.Sc. (Petroleum and Natural Gas Engineering) from Istanbul Technical University, Turkey • B.Engg. (Petroleum and Natural Gas Engineering) from Mehran University of Engineering and Technology, Pakistan • Attented Public College Hyderabad, Pakistan